

MASTER

The Solid State Chemistry of Rare Earth Oxides

RESEARCH CONDUCTED ON ATOMIC ENERGY COMMISSION CONTRACT

AT (11-1)-1109

TECHNICAL PROGRESS REPORT

1967 — 1968

LEROY EYRING

MICHAEL S. JENKINS VOLKER SCHERER

G. DUANE STONE

RHEAL P. TURCOTTE

JOYCE M. WARMKESSEL

GARY R. WEBER

ARIZONA STATE
UNIVERSITY
Tempe, Arizona

DISTRIBUTION OF THIS DOCUMENT IS UNLIMITED

DISCLAIMER

This report was prepared as an account of work sponsored by an agency of the United States Government. Neither the United States Government nor any agency Thereof, nor any of their employees, makes any warranty, express or implied, or assumes any legal liability or responsibility for the accuracy, completeness, or usefulness of any information, apparatus, product, or process disclosed, or represents that its use would not infringe privately owned rights. Reference herein to any specific commercial product, process, or service by trade name, trademark, manufacturer, or otherwise does not necessarily constitute or imply its endorsement, recommendation, or favoring by the United States Government or any agency thereof. The views and opinions of authors expressed herein do not necessarily state or reflect those of the United States Government or any agency thereof.

DISCLAIMER

Portions of this document may be illegible in electronic image products. Images are produced from the best available original document.

TECHNICAL PROGRESS REPORT

of

THE SOLID STATE CHEMISTRY OF RARE EARTH OXIDE SYSTEMS

LeRoy Eyring

Michael S. Jenkins Volker Scherer

G. Duane Stone

Rheal P. Turcotte

Joyce M. Warmkessel

Gary R. Weber

LEGAL NOTICE

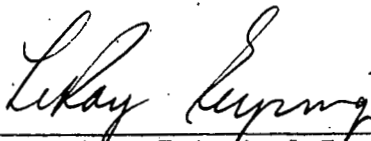
This report was prepared as an account of Government sponsored work. Neither the United States, nor the Commission, nor any person acting on behalf of the Commission:

A. Makes any warranty or representation, expressed or implied, with respect to the accuracy, completeness, or usefulness of the information contained in this report, or that the use of any information, apparatus, method, or process disclosed in this report may not infringe privately owned rights; or

B. Assumes any liabilities with respect to the use of, or for damages resulting from the use of any information, apparatus, method, or process disclosed in this report.

As used in the above, "person acting on behalf of the Commission" includes any employee or contractor of the Commission, or employee of such contractor, to the extent that such employee or contractor of the Commission, or employee of such contractor prepares, disseminates, or provides access to, any information pursuant to his employment or contract with the Commission, or his employment with such contractor.

APPROVED:



LeRoy Eyring, Principal Investigator

Gilbert L. Cady, Vice President

Arizona State University
Tempe, Arizona
July 10, 1968



TABLE OF CONTENTS

	Page
Synopsis of Technical Progress 1967-68.....	1
A Detailed Tensimetric Study of the Praseodymium Oxide-Oxygen System.....	6
Mass Transport Properties of Rare Earth Oxides.....	36
High Temperature X-ray Diffraction Studies.....	65
Experimental Program for Crystal Growing of Rare Earth Oxides.....	87

ADDENDUM TO PROGRESS REPORT

(Included separately)

Preprints

- "Phase Relationships in the Composition Range Between $\text{PrO}_{1.500}$ and $\text{PrO}_{1.714}$," Joyce M. Warmkessel and LeRoy Eyring. COO-1109-40
- "Optical Absorption Spectra of the Ordered Phases in the Praseodymium Oxide-Oxygen System," Joyce M. Warmkessel, S. H. Lin and LeRoy Eyring. COO-1109-41
- "On the Rare Earth Dioxymonocarbonates and Their Decomposition," Rheal P. Turcotte, James O. Sawyer and LeRoy Eyring. COO-1109-42
- "On the Rare Earth Carbonate Systems: The Normal Carbonates," Paul Caró, James O. Sawyer and LeRoy Eyring. COO-1109-43
- "Preparation and X-ray Studies of the Monocarbonates of the Lanthanide Elements," J. O. Sawyer, P. Caró and L. Eyring. COO-1109-44
- "A Note on the Decomposition of Rare Earth Nitrates," Paul Caró and LeRoy Eyring. COO-1109-45

In Press

- "Terbium," LeRoy Eyring. COO-1109-27
- "Praseodymium," LeRoy Eyring. COO-1109-28
- "High Temperature X-ray Diffraction Studies of the Terbium Oxide-Oxygen and Mixed Cerium, Terbium Oxide-Oxygen Systems," D. Arthur Burnham, LeRoy Eyring and J. Kordis. COO-1109-32
- "Phase Transformations in the Praseodymium Oxide-Oxygen System: High Temperature X-ray Diffraction Studies," D. Arthur Burnham and LeRoy Eyring. COO-1109-33
- "Self-Diffusion of Oxygen in Neodymium and Samarium Sesquioxide," G. D. Stone, G. R. Weber and L. Eyring. COO-1109-39

Reprints

- "Fluorite-Related Oxide Phases of the Rare Earth and Actinide Elements," LeRoy Eyring. COO-1109-26
- "On the Ternary System Samarium-Nitrogen-Oxygen and the Question of Lower Oxides of Samarium," T. L. Felmlee and L. Eyring. COO-1109-29
- "Some Tensimetric Studies in the Mixed Ceria-Terbium System," J. Kordis and L. Eyring. COO-1109-30
- "A Tensimetric Study of the Terbium and Praseodymium Systems and the Mixed Praseodymium-Terbium System," J. Kordis and L. Eyring. COO-1109-31
- "On the Possible Role of Dislocations in Generating Ordered and Disordered Shear Structures," J. S. Anderson and B. G. Hyde. COO-1109-34
- "Phase Relationships in the Americium-Oxygen System," T. D. Chikalla and L. Eyring. COO-1109-36
- "Dissociation Pressures and Partial Thermodynamic Quantities for Americium Oxides," T. D. Chikalla and L. Eyring. COO-1109-37
- "The Curium-Oxygen System," T. D. Chikalla and L. Eyring. COO-1109-38

SYNOPSIS OF
TECHNICAL PROGRESS
1967-68

This report consists of accounts of studies presently being conducted, preprints of completed work, manuscripts of papers submitted for publication, and reprints of articles which have been published since the last report. In many cases these results have been communicated orally both formally and informally at conferences and meetings.

The locus of this research moves among studies of reactions involving solids. For the most part attention has been focused on the solids themselves, yet these reactions usually involve a gas phase in equilibrium, permitting changes in composition by variation of temperature or pressure of the system.

These studies continue to center around the rare earth oxides and carbonates because they present a strategic window through which solid state behavior may be viewed. As model systems they exhibit ordered phases of narrow composition limits (frequently showing polymorphism) as well as truly nonstoichiometric phases of wide composition range.

These features may be modified at will by a shift of attention to various members of the series or by a discriminating admixture which changes the system in some subtle way.

The similarity between contiguous phases is so great in some cases that one witnesses the unusual behavior of materials variously termed hybrid crystals, coherently intergrown crystals, domain structures,

pseudophases and grossly nonstoichiometric compounds. When these substances are understood, a giant stride toward knowledge of solid state behavior shall have been taken.

This research relates directly to the efforts of the Commission in several important ways. There are uses of rare earth oxides in nuclear applications, including energy sources. The rare earth oxide systems are of the same family of oxides as those of the actinide elements hence the importance of a parallel study, both since the actinide oxides are themselves important reactor fuels and energy sources and the need for knowing the general chemistry of the transplutonium elements whose availability is increasing rapidly. Even more important in the long run, these studies shall contribute to the extension of knowledge of the nature of solids, a subject of unending practical and theoretical interest to the Commission.

As a result of intense activity over the past thirty years it can be argued that the chemistry of materials only slightly defective or nonstoichiometric is well understood. This applies where point defects are the most important species present. Materials having extended defects or gross nonstoichiometry, however, are almost an uncharted wilderness. Whereas the theories of Schottky, Wagner, and Frenkel were instrumental in bringing understanding of materials with point defects and therefore stimulated the development of practical and theoretical techniques of dealing chemically with them, there is no comparable development for grossly defective materials. The situation is not unlike the studies of the theory of liquid solutions where dilute solutions are usually thought to be well understood, but concentrated ones less so, except that in the case of solids one must reckon with the increased complexity of a phase

capable of all the complex atomic interactions of concentrated solutions yet adding the further complications of phase transformations, hysteresis and the like.

In fact, there has not even been a complete catalog or classification of the varieties of phases possible in grossly defective solids. Such entities or phenomena as dislocations, stacking faults, defect clusters, domains, microheterogeneity, order-disorder transitions, premonitory effects, hysteresis, and pseudophase formation figure prominently in the chemical and physical properties of these materials. A vast experimental effort on the structure, thermodynamic properties and transport properties of these materials must be associated with a sound theoretical development if understanding is to come.

Tensimetric Studies on Oxides.--The exploitation of the powerful isobaric technique of studying oxygen pressure, temperature, and oxide composition has been continued (pp 6-35) to extend our knowledge of equilibrium, nonequilibrium, and pseudophase regions of the praseodymium oxide-oxygen system. The apparatus has been improved and equilibrium measurements are yielding precise thermodynamic data for the grossly nonstoichiometric alpha phase. The results of this study are scheduled for presentation at the Seventh Rare Earth Research Conference in San Diego in October.

High Temperature X-ray Studies.--Concomitant with the tensimetric studies of the pseudophase region is an exploration (pp 65-86) of high temperature X-ray diffraction techniques to reveal structural changes in the phase regions contiguous to iota which demonstrate interesting reversals, bivariant behavior and marked hysteresis.

The high temperature diffractometer is also being used to investigate the steps in thermal decomposition of oxalates (see preprint C00-1109-42) and formates. Current results were presented at the annual meeting of the Arizona Academy of Science at Flagstaff in May 1968 and will be given at the National Meetings of the American Chemical Society in Atlantic City in September.

Oxygen Transport in Rare Earth Oxides.--Surface reaction and diffusion properties of oxygen in rare earth sesquioxides have been studied and the results for Nd_2O_3 , Sm_2O_3 and Er_2O_3 reported at a conference on Mass Transport in Oxides held in October 1967 at the National Bureau of Standards (C00-1109-39).

A study of oxygen diffusion in the phase $\text{Pr}_7\text{O}_{12+6}$ is progressing (see pp 36-64). This research observes the temperature and pressure dependence of the diffusion coefficient and correlates these with tensimetric measurements. It is hoped to clarify the energetics and mechanism for the diffusion and reaction process for this stable intermediate phase of narrow composition range. Results so far obtained were discussed at the Flagstaff meeting of the Arizona Academy of Science in May 1968.

Optical Absorption Measurements on PrO_x Phases.--The optical absorption spectra in the visible and ultraviolet region for the A- and C-form Pr_2O_3 have been recorded and tentative assignments made for the transitions observed. In addition, the near infrared spectra for the intermediate phases of the $\text{Pr}_n\text{O}_{2n-2}$ series were recorded and discussed in C00-1109-41 and were presented at the National Meeting of the American Chemical Society in San Francisco in April 1968.

Crystal Growth of Rare Earth Oxides.--A program aimed at producing single crystals of the higher oxides of the rare earth elements, especially the intermediate phases of the homologous series $\text{Ln}_n\text{O}_{2n-2}$ has been pursued without final success. The results obtained so far are given in the report, page 87 and following. It has been possible to grow nice small crystals of CeO_2 , but praseodymium in the trivalent state either forms compounds with the fluxes tried under the conditions of our experiments or produces the A-type sesquioxide which breaks up when it is oxidized.

General lectures and/or discussions on the solid state chemistry of rare earth oxides were presented at Battelle Northwest in Richland, Washington in August 1967, Asilomar High Temperature Conference in September 1967, the University of Freiburg, Oxford and Rome, the Bellevue Laboratories in Paris, the Euechem Conference on High Temperature Chemistry at Semmering in September and October 1967. A paper on phase transformation in the iota region for pure and mixed rare earth oxides was given at a Materials Science Center Dedication at the University of Missouri at Rolla in October 1967.

A DETAILED TENSIMETRIC STUDY
OF THE
PRASEODYMIUM OXIDE-OXYGEN SYSTEM

The praseodymium oxide-oxygen equilibrium is becoming an important model system of substances exhibiting gross nonstoichiometry in the solid phase. The chief goal of this research has been to derive reliable thermodynamic data for this system. Consequently some time has been spent in ascertaining the equilibrium conditions necessary to produce such data. Two important factors governing the attainment of equilibrium have been discussed in a previous report.¹ Details were also given of the modifications made to the existing apparatus to suit the new experimental conditions. Further improvements are described in this report and a preview is given of the modifications to be carried out in the near future.

As is to be expected, such detailed investigations have uncovered various other small related problems. Where relevant, these were pursued and the results of such research are described in the appropriate section below.

I.

Experimental Conditions Necessary to Attain
True Thermodynamic Equilibrium
in the Praseodymium Oxide-Oxygen System

It was observed as a result of several isobars carried out at the same pressure that occasionally a plot would be obtained that exhibited marked differences from what was accepted as being the normal behavior

of the system. Such anomalous behavior could usually be related to the fact that a new oxide sample was used, i.e., one which has been subjected to only one reduction to the sesquioxide followed by oxidation to $\text{PrO}_{1.833}$. In all cases in these experiments, vacuum reduction was used to obtain the sesquioxide. The behavior of praseodymium oxide with increasing numbers of isobaric runs is discussed in detail in section VII.

Work carried out on a Norelco high temperature X-ray unit indicated that the temperature of a thin bed of oxide (as measured by an optical pyrometer) was lower than that measured by an adjacent Pt/Pt-10% Rh thermocouple by about 3%. Emissivity corrections could easily be applied to a thin bed of sample; however, in this case the sample was contained in a platinum bucket 2.5 cms x 1 cm. In order to ensure that any temperature gradient across the sample should be minimized, a platinum lid was suspended over the top of the bucket, reflecting the radiation from the top of the sample and positioned so as not to produce a pressure gradient across the sample, i.e., the reacting oxygen had easy access to the oxide.

Previous work had indicated the desirability of a slower rate of heating and cooling than 1.3° per minute.² Very slow manually controlled runs had shown slight differences from runs carried out at 1.3° per minute. These, however, suffered from the defect that the temperature increments could not be made small enough to give a smooth heating and cooling curve. Consequently, two clock motors were installed together with suitable gearing, enabling isobars to be determined at rates varying from 0.02° to 0.8° per minute.

Results.--A series of experiments were conducted in which each of the parameters previously described was varied independently and the effects produced (if any) were compared with similar isobars determined

by previous workers. The nomenclature used in describing the various portions of these relatively high pressure isobars is shown in Figure 1.

In Run 4, the bucket (containing a new sample) was covered with a platinum lid and the run carried out at a rate of $\sim 1.3^\circ/\text{min}$ with an oxygen pressure of 637 mm which was not controlled. The heating curve was found to agree with that of corresponding isobars previously determined with uncovered buckets. At 476° β transformed to α (see Figure 1), and the isobaric path lay on the α surface up to 805° , at which temperature α reduced to $z + \alpha$. At this pressure the conversion to z is slow and, in fact, never reaches completion (see section II). At 1046° , the αz pseudophase was seen to reoxidize across the descending $z + \alpha$ blade in complete agreement with previous workers. At 1060° α decomposed to σ at a composition of $\chi \approx 1.693$ and σ persisted until the highest temperature 1120° was reached.

On cooling, the isobar showed normal behavior until a temperature of 1060° was reached. Previous work had indicated that at this point, the oxidation product is α which then becomes metastable with respect to αz on reducing the temperature. On cooling further, a gradual conversion of α to αz is usually seen. In this case, however, Figure 1 shows that the cooling path lay on the projected α surface with little or no conversion to αz . It seemed, therefore, that a reduction of temperature gradient across the sample had stabilized α , since the rate of heating and cooling was the same as that used by previous workers. It should be emphasized at this point that the oxide sample was a new one, i.e., it had been subjected to only one reduction and reoxidation.

Run 5 was carried out in an identical manner and again α seemed to be stable with very little conversion to αz . For Run 6 the platinum lid,

which was the only feature differing from the conditions used by previous workers, was removed to see if their isobars could be duplicated. The rate of heating and cooling and the pressure was kept the same. It was found that the isobaric path traced out on cooling more closely resembled that found by previous workers.

With the lid still removed from the bucket, Run 7 was carried out at a rate of 0.5°/min. Even with the slower rate it was found that the behavior of the isobar increasingly approached those of previous workers with increasing number of runs. It was now becoming apparent that the history of the sample was important. As a result, the series of experiments described in section VII were thought to be of value in gaining a better understanding of the praseodymium oxide-oxygen system.

Previous studies had shown the desirability of using slower rates of heating and cooling than 1.3°/min since there was doubt concerning the attainment of equilibrium under the forced pace of temperature change at this rate, particularly in the pseudophase region. During Run 8 ($p_{O_2} = 637$ mm, rate 1.3°/min, without lid), the run was halted during the cooling cycle at 854° to test for equilibrium in the αz region. A drift toward z was observed corresponding to a weight decrease of ~ 1.5 mg, i.e., a stoichiometry change of ~ 0.006. The final "equilibrium" composition reached, however, was 1.732, which was well to the right of 1.714, showing that in this region transformation of metastable $\alpha z \rightarrow z$ was unlikely to occur.

This drift towards z on cooling had not been previously observed and the weight loss of 1.5 mg in this region would require, under forced conditions, a temperature change of about 150° to effect the same change in stoichiometry. It is interesting to note that although this region

is not at thermodynamic equilibrium, the sample was at all times in equilibrium with respect to temperature. Careful analysis of the weight versus temperature chart showed that small temperature fluctuations (both up and down) produced a corresponding decrease or increase in weight. These small variations were superimposed on a general drift to a lower oxide composition.

It was decided at this stage that it would be useful to determine the reproducibility of an isobaric run, since experiments 4, 5, and 6 had shown the sample history to be important. Runs 9, 10, 11 and 12 were carried out at the same rate and oxygen pressure ($1.3^\circ/\text{min}$, $p_{\text{O}_2} = 637 \text{ mm}$), which was controlled using the automatic pressure controller (APC). These experiments showed that after a minimum number of runs, about four, the isobaric path, at a given pressure, was reproducible. It was found on superimposing any two isobars that the temperatures at which the phase boundary reaction occurred were in excellent agreement, while slight variations were observed in the pseudophase region. This is to be expected since the system is not at thermodynamic equilibrium in this region. Even so, the variations when two consecutive runs were superimposed were even smaller.

On comparing Runs 9-12 with equivalent isobars determined by previous workers, it was observed that the heating and cooling paths in the α region were now coincident, whereas previously the cooling path was seen to lie above the heating path on the α surface, as shown in Figure 1. Various runs up to Run 9, during which the pressure was not controlled, had shown the displacement of the heating and cooling paths in the α region. It should be mentioned at this point that together with this coinciding of the up and down paths in this region, a slight zero

displacement was observed of ~ 0.25 mg. This zero displacement, although considered at the time to be some zero drift of the balance, was to become of greater significance later (see section III). This zero shift corresponded to a compound being formed of composition slightly greater than $\text{PrO}_{1.833}$, i.e., the cooling path of β lay to the right (higher oxidation) of the heating path. Run 13, during which the oxygen pressure was not controlled, also showed no divergence in the α region, i.e., there was no apparent difference between a pressure controlled and uncontrolled run. Some greater differences were observed in the hysteresis region αz for the uncontrolled run.

The effect of using a slower rate than $1.3^\circ/\text{min}$ was investigated in Run 14. This experiment, carried out at $0.45^\circ/\text{min}$, showed that there was no significant difference between the slower and faster run. During the latter half of the experiment, i.e., when traversing the lower half of the α region on cooling, the rate was increased to $\sim 1.3^\circ/\text{min}$. This produced a greater divergence between the heating and cooling paths than for the slower part of the run. Again the isobaric paths of Run 13 and the previous runs were not quite superimposable in the pseudophase region. This was also confirmed by Runs 15 and 16. In Runs 9-16 a slight displacement of the β phase was observed, putting it further to the right with each run.

For Runs 17 and 18 the platinum lid was replaced on the bucket to see whether the dramatic difference in the αz region observed in Runs 4 and 5 could be reproduced. For both runs $p_{\text{O}_2} = 637$ mm and was controlled by the APC. In Run 17, the rate of heating was $1.3^\circ/\text{min}$ while the rate of cooling was slower, at $0.45^\circ/\text{min}$. The rates of heating and cooling were constant in Run 18 at $1.3^\circ/\text{min}$. In both these runs isobars were

obtained which were different in the α region from those produced in Runs 4 and 5, but which resembled very closely those obtained in Runs 6-16, i.e., they showed "normal" behavior in this region. Run 19 was run as a check without the APC so that Runs 4 and 5 could be exactly duplicated. This again failed to produce the effects seen in Runs 4 and 5.

To recapitulate, improvements to the apparatus used in the isobaric studies, i.e., automatic pressure control, slower rates of heating and cooling, reduction of any temperature gradients across the sample, conclusively showed that with this method of recording temperature and weight changes on the chart paper, no significant differences were to be detected by varying the experimental conditions in the manner described. However, these experiments did show that sample history seemed to be important when considering the reproducibility of any two isobars. The greater the number of experiments to which the sample was subjected, the greater the reproducibility, even in the pseudophase region. These experiments were of great value in ascertaining the optimum experimental conditions necessary for obtaining accurate thermodynamic data described in section V.

II.

Investigation of Equilibrium Conditions in the Pseudophase Alpha-Iota Region

During the course of Run 8 an initial investigation was made to see whether the isobaric path traced out represented the equilibrium path in this region. Run 8 was halted during the cooling cycle at a suitable temperature in the α region for a period of about 12 hours. The results are discussed in section I.

Run 20 was commenced under optimum experimental conditions (discussion in previous section) at a pressure of 637 mm of oxygen. Heating

was continued normally until a temperature of 840° was reached. Up to this point the α surface traced out was perfectly superimposable on α surfaces generated during previous runs. The temperature programmer was switched off and the system was allowed to reach equilibrium at this temperature. Figure 2 shows the "equilibrium" isobaric path traced out under these conditions. The sample was maintained at a given temperature until its weight, as indicated on the chart recorder, did not decrease further with time. The time taken for this to occur is indicated in the diagram. Figure 2 shows that the "equilibrium" path lies below the isobaric path under forced conditions and that during the first 36 hours a weight loss of 9.5 mg occurred. The sample was at all times in equilibrium with respect to temperature since it responded almost immediately to very small fluctuations in furnace temperature. These small changes were superimposed on a general drift towards regions of lower stoichiometry. After this initial period of about 36 hours, further loss in weight with time was extremely small, and the composition of the sample was always well to the right of 1.714. During the next three days the temperature was increased slowly to 870° . After each incremental adjustment the sample came rapidly to equilibrium and showed only very small decreases in weight with respect to time of the order of 0.5 mg or less. One very interesting feature that became apparent as a result of this experiment was that up to a temperature of $\sim 940^{\circ}$ any drift observed was always towards *iota*, i.e., towards a lower stoichiometry. Above this temperature up to 1050° any drift was always away from *iota*, towards a region of higher oxygen content. The mechanism of the $\iota \rightleftharpoons \alpha \rightleftharpoons \alpha$ equilibrium observed in this region has been discussed previously.^{2,12} It is possible to conclude that below 940° *iota* becomes more stable with

respect to alpha. When in the temperature range 940°-1050°, alpha is the more stable species. This experiment defines more closely the equilibrium between the two phases and pseudophase in this temperature range and shows that although thermodynamic equilibrium is not to be expected in this region, differences are observed between "equilibrium" isobars and isobars executed at 1.3°/min. The reversal observed at about 1050°, which is characteristic of isobars at this pressure, also showed interesting details which were not apparent at a faster rate of heating.

On cooling the temperature from 1050° to 920°, any drift in composition was towards iota, which is to be expected since metastable $\alpha \rightarrow \alpha\prime \rightarrow \iota$. Again the weight change was very small and the sample rapidly came to "equilibrium" in this temperature range. The total time taken to complete the run was about four weeks. One very distinguishing feature that became apparent as soon as the temperature was low enough to begin describing the α surface was that the heating and cooling paths of α were displaced about 2.5 mg. This displacement was continued until $\alpha \rightarrow \beta$ at about 420°. Consequently, the β phase, on cooling, was shifted to the right of the β traversed on heating. It was thought initially that this shift was some mechanical artifact, e.g., it is possible that the balance beam could have slipped on the knife edges. The results obtained, however, were interesting enough to justify another long run.

Similar fine details were observed in Run 21 in the pseudophase region. Again a zero displacement was observed on returning to β . This time the beam arresting facility incorporated in the balance was employed to lift the beam off the knife edges. Upon again releasing the beam, the zero was noted and found to coincide with the displaced β phase. This zero displacement, therefore, was unlikely to be mechanical in nature,

which immediately posed the question of a possible reaction between the oxide and its platinum container.

Due to the time taken to complete a detailed investigation of this region and due to the zero shift when the sample was subjected to elevated temperatures for considerable periods of time, the project was abandoned, at least temporarily.

III.

Investigation of the Reaction of Platinum with Praseodymium Oxide

Evidence is cited in section II which suggests that prolonged heating of praseodymium oxide in contact with platinum at elevated temperatures causes some chemical reaction to occur which is manifest as a zero shift in the β phase. Experiments carried out later showed conclusively that this was not due to a mechanical or electrical defect in the weight-measuring unit. The best evidence for this was that during runs of similar duration, but without involving such high temperatures, i.e., $< 820^\circ$, the zero for the β phase was always coincident. After reducing the sample again to the sesquioxide, the zero for $\text{PrO}_{1.500}$ in vacuum was compared with the zero for the same sample after the initial reduction. It was found that the zero after the second reduction was 1.7 mg heavier than was originally observed. It would appear, therefore, that by reacting with platinum some species had been produced which was not completely reducible. At the other end of the scale used for calibration, i.e., the β phase, it appeared that the platinum, by reacting with the oxide, was converted into some form which was now capable of oxygen uptake, which would account for the shift of the β phase zero towards regions of higher oxygen content. If some mechanical shift had occurred, one might

expect the zero for $\text{PrO}_{1.500}$ to be shifted by the same amount as that of $\text{PrO}_{1.833}$. Since this did not occur it was concluded that a reaction had taken place between the oxide and its platinum container.

The oxide was removed from the bucket, which was then washed in dilute HNO_3 to remove any trace of oxide, followed by washing with distilled water. After drying, the bucket was weighed and when this weight was compared with the original weight, it was found that the bucket had lost 28.6 mg of platinum. The washing in dilute HNO_3 was repeated, but no further loss of platinum occurred. Calculations based on the work of W. L. Phillips,³ who studied the oxidation of platinum metals, showed that the maximum weight loss that could be expected from a bucket of these dimensions due to volatile oxides was about 5 mg.

An experiment was carried out in which the bucket was boiled to constant weight in HNO_3 and heated for one month at 1000° so that the rate of loss of platinum when not in contact with praseodymium oxide could be determined. This was found to be ~ 0.1 mg. The loss of 28.6 mg of platinum could only have been due to its reaction with the oxide.

This shift in β composition had not been observed by previous workers presumably because the time spent at elevated temperatures was much shorter than for Runs 21 and 22. A close scrutiny of their zero for $\text{PrO}_{1.833}$ over a long series of runs showed it to be constant within the limits of experimental error. Indeed, it has been previously mentioned, this shift was only observed for runs lasting about one week; the zero for short runs, i.e., ~ 3 days, was always found to be constant. This reaction of platinum with the oxide is thought to be a very subtle one, having little or no effect on the overall interpretation of the $\text{PrO}_x\text{-O}_2$ phase diagram. This was shown to be so by using an alumina bucket to contain the oxide.

Experiments had shown the reaction between alumina and PrO_x to be much less than that observed with the platinum container. Isobars determined in this way were seen to be identical to those obtained by previous workers using a platinum container and a faster rate of heating. Consequently, their interpretation of the overall reaction in terms of the various phase reactions remains unchanged.

Emission spectroscopy was used to try to identify any platinum present in the oxide used in the experiments. The emission spectra of the rare earth elements are very complex and tend to obscure even the strongest platinum lines, making identification of any platinum very difficult. In order to facilitate such an identification, a series of seven spectra was taken consecutively on the same film in the following order:

Pt	PrO_x	Fe	Fe	PrO_x	PrO_x	PrO_x
	Doped with Pt	Standard	Standard	Pure	Sample used	Doped with Pt

Proceeding in this manner, the 2659 platinum line was seen to be present in both the sample taken from the platinum bucket and doped sample, but absent in the pure oxide sample. Tentative estimates of the percentage platinum showed it to be present in amounts $< 0.1\%$. The low percentage of platinum may be accounted for by the fact that the platinum was not evenly distributed throughout the oxide. X-ray fluorescence was also tried to identify any platinum present, but again the spectrum of the oxide completely obscured the platinum peaks.

The net result of this study was to show that there was reasonable evidence for believing that the oxide reacted with the platinum at elevated temperatures and relatively high oxygen pressures. This was avoided in later studies by using an alumina bucket in which the reaction was very much less.

IV.

Investigation of Apparent Discrete Steps
in the Oxidation-Reduction Cycle

Isobars executed at rates of about $0.5^\circ/\text{min}$ appeared to show small discrete steps in the α region. These steps formed closed loops upon ascending and descending the σ region. When examined in detail, the steps were found to be of the order of 0.1 mg per 4° which seemed to be greater than the variation that could be accounted for by a purely mechanical factor since the effect of temperature variation or slide wire sticking could be readily estimated from the horizontal portions of the isobar. In the horizontal regions, the steps appeared to be half the magnitude of the steps in question. It was of interest to investigate these features more closely since similar effects had been observed by Elliott and Lemons⁴ in their work on the cerium-cadmium system. Roof and Elliott⁵ also quote X-ray diffraction evidence for microphases in $\text{CeCd} \sim 4.5$ solid solutions. If the steps in the praseodymium oxide-oxygen system were real, then one might invoke a similar explanation in this system, i.e., a microhomologous series involving discrete microphases.

Initial exploratory experiments had shown the desirability of improving the weight and temperature measurement by a factor of ten so that any steps present might be clearly visible. The sample weight was increased from 2 to about 8 g and was contained in a compound alumina bucket consisting of a smaller bucket inside a larger one. By this means the bed depth of the oxide was kept small so that both temperature and pressure gradients across the sample were minimized. The smaller bucket was supported on an alumina post so as to ensure free oxygen access

to the sample and the top of the upper bucket was loosely covered with a platinum lid. The temperature was measured manually by connecting the thermocouple leads to a very sensitive potentiometer, type K-3 Universal Potentiometer manufactured by the Leeds and Northrup Company, capable of measuring to 1×10^{-4} m.V. Such sensitive temperature measurements required the design of a new and larger furnace so that temperature gradients across the sample could be minimized.

The heating element was made by winding heavy gauge Kanthal wire around a two-foot alumina core, making the total resistance about 10 ohms. An Inconel pipe 18 inches by 2 inches diameter was placed inside the alumina core immediately surrounding the quartz hang-down tube of the Ainsworth balance. A larger 18 inch by 5 inch diameter Inconel pipe was placed around the alumina core and the inner pipe to act as a heat sink, minimizing temperature gradients that could arise due to hot spots on the Kanthal windings. The furnace profile was determined, using a NBS Calibrated Pt/Pt-10% Rh thermocouple. The sample was placed in a 4 inch zone in the furnace across which the temperature drop was 1°. Since the sample bucket was less than two inches long, the temperature gradient across it was assumed to be better than this.

Results.--A suitable portion of the α region was chosen, i.e., one which had exhibited steps during a slow isobaric run which was recorded on chart paper. The temperature range chosen was 518°-732° and was traversed both up and down during a period of about five days, giving a heating and cooling rate of 0.08° per minute. The oxygen pressure was set at 638.9 mm and the temperature was recorded every time the sample weight changed by 0.1 mg.

Examination of the isobaric paths plotted showed no evidence whatsoever for discrete steps in the α region. That such steps were in evidence when the run was automatically recorded could only mean that they were due to some periodic function of the apparatus. However, the experiment was of value since it showed that:

1. The α surface was curved. It was found to be convex with respect to the temperature axis, which had been proposed in the original work on the system² but was not really evident in the faster runs.

2. The conditions necessary to produce meaningful thermodynamic data in this region could be accurately defined. A very interesting feature of this study was that it showed, even at this slow rate of heating, that there was a displacement in the heating and cooling curves in the α region. This displacement (corresponding to a change in stoichiometry of 0.0002) would be impossible to detect using the chart recorder. Moreover, the displacement was always that the cooling path lay below the heating path, which was exactly opposite to what had been seen during faster runs. When the run was halted during the heating cycle to test for equilibrium, the path traced out was as shown in Figure 3, (1). During the initial, relatively rapid rate of cooling, the cooling path approximated to the cooling path at a rate of $0.08^\circ/\text{min}$, i.e., curve B. Eventually the temperature controller settled down and the true equilibrium path described was located almost exactly halfway between the heating and cooling curves. A similar effect was observed when the run was halted during the cooling cycle, i.e., the path traced out corresponded to Figure 3, (11). The experiment showed that if an infinitely slow rate of heating and cooling were employed, for each pressure, a unique isobaric path would be traced out in the α region.

V.

Evaluation of Thermodynamic Data

in the Alpha Region

The main effort of research is now being directed along these lines. The information acquired will be compared with the thermodynamic data derived for related systems.^{6,7,11}

Experiments carried out in section IV indicated that if meaningful thermodynamic data were to be obtained for this region, then the temperature would have to be monitored manually. A rate of heating and cooling of about 0.1° per minute, however, would be prohibitively slow. A series of experiments were therefore carried out in which the rates of heating and cooling were varied from ~ 0.08° per min to 0.8° per min and the effect on the displacement of the isobaric path in the α region observed. It was finally decided that the optimum rate should be 0.45° per minute. The thermocouple EMF was measured, using a Minneapolis-Honeywell potentiometer, reading to 1×10^{-4} m.V. The oxygen pressure was controlled to ± 0.1 mm, using the Granville-Phillips APC. At the completion of each run a sample of oxygen was tested on a mass spectrometer to ensure no leak had occurred during the experiment.

Results.--A series of 12 isobaric runs are planned in the pressure range 190-760 mm, of which six have been completed. Figure 4 shows a plot of the relative partial molar free energy versus temperature for various constant values of x in PrO_x at 0.005 O/Pr intervals. The relative partial molar free energy is a measure of the work done in transferring one mole of oxygen from the gaseous phase of standard pressure to the non-stoichiometric oxide at a pressure of p atmospheres. The relative partial molar entropy of solution of oxygen is given by

$$\bar{\Delta S}(\text{O}_2) = -[\partial \bar{\Delta G}(\text{O}_2) / \partial T]$$

while the relative partial molar enthalpy may be evaluated from the expression

$$\bar{\Delta H}(O_2) = \partial(R \ln p_{O_2}) / \partial(1/T)$$

Figure 4 shows a greater scatter at the compositions nearest the stoichiometry of the δ phase. Although the data is not complete, initial estimates of $\bar{\Delta S}(O_2)$ are of the order of 100-160 cal $^{\circ}K^{-1}$ mole $^{-1}$, showing that the mechanism of solution of oxygen in this system bears a close similarity to that in the CeO_x-O_2 system.

Concurrent with this detailed investigation of the α region, some isobaric runs were continued up to 1100 $^{\circ}$ so that integral molar quantities could be calculated for this system. However, it has been recently observed that repeated exposure of the sample in the alumina bucket to long periods of time at elevated temperatures causes a slight reaction between the oxide and its container. Despite the fact that the amount of reaction is far smaller than that observed for the platinum bucket under similar conditions, it causes some difficulty in the assignment of the stoichiometry of the sample. The continuation of the runs to higher temperature has now been halted and under these conditions, there is no evidence for any reaction between the oxide and its container.

X-ray powder photographs were taken of the oxide samples which had been in intimate contact with the alumina bucket. Comparison of this film with others taken of pure oxide showed no extra lines due to the possible formation of praseodymium aluminate. It is possible that since the reaction is so slight, the reaction product is present in amounts too small to be detected. Another container is being sought so that similar work can be carried out at higher temperatures.

Modifications to the temperature and weight recording system are planned in the near future so that the process can be automated without any loss in sensitivity. A digital voltmeter, Model 6653 manufactured by Lear Siegler Corporation, has been purchased so that the weight and EMF change can be monitored simultaneously at predetermined time intervals. The output is to be fed to a model 2301 Flexowriter with tape punch, manufactured by the Friden Corporation. Each run, therefore, will be recorded on paper tape for a permanent record, while the printout facility will enable each run to be monitored instantly. This arrangement permits maximum flexibility, since in the future it is hoped to interface the punched tape with a computer which would be programmed to calculate the required data.

VI.

Experiments to Investigate the Effect of Limiting Microdomain Size on the Praseodymium Oxide-Oxygen Phase Diagram

The behavior of the praseodymium oxide-oxygen system has been adequately explained in terms of the microdomain theory, and similar explanations have been invoked to explain the way other oxide systems react (see section II). In the $\text{PrO}_x\text{-O}_2$ system, the domain texture is thought to be fine and of the order of about 20 Å. The object of this research is to prevent, in some suitable manner, the intergrowth of these domains. If this could be achieved, then it is possible that a dramatic effect would be observed during the course of an isobaric run; for example, in the oxidation of $\sigma \rightarrow z$ where σ is thought to be eventually eliminated by the expansion of the z microdomain boundaries.

A means was sought of suspending the oxide in a medium which would limit growth along any axis to less than 20 Å. Linde molecular sieves were tried as a suitable suspending medium. Molecular sieves are generally alkali metal aluminosilicates similar to many natural clays and feldspars. When the water of hydration is driven off, the crystal does not collapse or rearrange, as is the case with most other hydrated materials. Instead, the physical structure of the crystal remains unchanged, which results in a network of empty pores and cavities that comprise about one-half of the total volume of the crystals. Various sieves are available having different pore sizes up to 13 Å. The size of a hydrated Pr^{+3} ion was estimated to be of the order of 6 Å, and so a 13 Å pore sieves was chosen as being suitable for suspending the oxide. This sieve has a cubic crystal structure $a_0 = 24.95$ Å characterized by a three-dimensional network with mutually connected intra-crystalline voids accessible through pores which will admit molecules with dimensions up to 13 Å. Unfortunately, this sieve is stable only in solutions of pH 5-12. Acid stable sieves are available, but the pore size in these is < 6 Å and so are unsuitable for accommodating Pr^{+3} ions.

$\text{Pr}(\text{NO}_3)_3$ was prepared by dissolving the oxide in concentrated HNO_3 and the pH adjusted to be $\sim 4-5$ by dilution with distilled water. About ten grams of molecular sieve were placed in a quartz tube whose open end was connected to the tube containing $\text{Pr}(\text{NO}_3)_3$. The nitrate was frozen in liquid N_2 and the whole system evacuated. A furnace was placed around the tube containing the molecular sieve and the temperature raised to about 350° in order to outgas the sieve. After the sieve had cooled to room temperature, the quartz tube was rotated, which allowed the sieve

pellets to fall into the nitrate solution which had also warmed to room temperature. Absorption of $\text{Pr}(\text{NO}_3)_3$ into the sieve pores was then assumed to take place.

After several hours, the sieve was removed and the pellets dried at 120° . This procedure was repeated several times. When the sieve was warmed up in vacuum, a blue species, N_2O_3 , was seen to condense out in the liquid nitrogen trap. This showed that the nitrate ion, at least, had entered the sieve lattice. After several dosings, the sieve was heated in a stream of oxygen, during which time it was hoped that all the $\text{Pr}(\text{NO}_3)_3$ suspended in the sieve would be converted to the oxide. Later weighing showed an increase in weight of the sample of 200 mg, hopefully corresponding to the retained oxide. This was far less than the amount of Pr^{+3} uptake expected, however, repeated dosings might induce further uptake.

Experiments are planned using a quartz spring in which the oxide suspended in the sieve is to be subjected to an isobaric study. Comparison of these results with previously obtained isobars on unsuspended oxide would reveal any difference due to limitation of domain growth. It is important to ensure that no chemical reaction takes place between the sieve material and the oxide, which might lead to erroneous conclusions. A control experiment is planned in which an intimately ground mixture of sieve and oxide are heated together. Since the oxide is not actually suspended in the sieve pores in this experiment, comparison with previous isobars should indicate whether or not a chemical reaction has taken place between the sieve material and the oxide.

VII.

Investigation of the Variation of the Surface Area
of Praseodymium Oxide

with Increasing Number of Reaction Cycles

Runs 4 and 5 (described in detail in section I) are two examples of a phenomenon that has been frequently observed during the course of this work, i.e., an isobaric run carried out on a fresh sample of PrO_x nearly always gave rise to unusual features, particularly in the hysteresis regions. After the sample had been subjected to about four such successive runs, these anomalies could never be reproduced. The fact that the anomalous behavior occurred in the hysteresis region $1.750 \leq \text{O/Pr} \leq 1.714$ was significant. Due to the stability of the microdomain texture in this region, the term "pseudophase" was adopted to describe its behavior.² The appearance of such a pseudophase required that there should be coherence between the reactant and product phase. Everett and Nordon⁸ suggested that lattice strain resulting from such coherence would cause hysteresis in phase transformations, conversely lack of coherence, as shown by a reduction in crystal size, i.e., an increase in surface area, would be expected to prevent hysteresis.

It had been observed in oxidation studies on TbO_x ⁹ that the chemisorptive capacity of the oxide surface towards oxygen decreased slightly over a series of runs until it reached a more or less constant value. The number of runs required for this to occur was generally found to be about five. BET measurements showed that the surface area decreased slightly with increasing treatment until it became fairly constant (within experimental error) after about five runs, probably due to sintering. Since the treatment of PrO_x in the isobaric work was almost identical to

21

that of TbO_x , it suggested that the anomalous behavior observed when a new sample of PrO_x was used--a behavior which was not reproducible--might be related to a small decrease in surface area due to sintering with increasing number of experiments.

Results.--A conventional gas adsorption apparatus was used for studying the adsorption of N_2 at -196° on the oxide surface. The equilibrium pressure was read using a telescope to ± 0.01 mm. Praseodymium oxide was freshly prepared by thermal decomposition of the oxalate at $\sim 800^\circ$. About 5 g of sample was placed in an adsorption bulb which was then attached to the vacuum system. Nitrogen was admitted in small doses to the sample and the process was continued until a final pressure of about 40 cms was reached. A typical adsorption isotherm is shown in Figure 4. The "point B" is clearly shown and the volume of gas adsorbed corresponding to monolayer coverage was estimated from the change in slope at this point. Several such values were checked by the BET plots using the equation:--

$$\frac{X}{V(1-X)} = \frac{1}{V_m C} + \frac{(C-1)X}{V_m C}$$

whose V_m = volume of gas adsorbed in 1 monolayer

X = reduced pressure P/P_0

V = volume adsorbed in $M^2 \cdot g^{-1}$

C = constant

For the first sample, two consecutive isotherms were determined in order to estimate the reproducibility of the surface area measurements. Although the actual value of the surface area could be in error by as much as $\pm 25\%$,¹⁰ the reproducibility was found to be as good as $\pm 2\%$. Excellent agreement was also found between surface areas determined by the "point B" method and BET plots.

After an adsorption isotherm had been determined on the sample, it was heated to 1100° in oxygen, simulating its behavior during an isobaric run. After cooling, the oxygen was pumped off and a second adsorption isotherm determined.

It was hoped to include a study of the oxide particles using an electron microscope, i.e., it was thought that the decrease in surface area might be due to an effective increase in particle size due to sintering. Consequently the average particle size, which could be estimated using the electron microscope, should increase. However, due to the density of the powder sample it was extremely difficult to observe single oxide particles. The particles tended to stick together in a random manner producing irregular clumps varying in size from 0.2 μ to 5 μ . An alcohol suspension was tried in order to separate single oxide particles but this was unsuccessful. This difficulty had also been observed during a similar study of TbO_x and no definite conclusion could be drawn from such measurements.

Four runs were carried out, each surface area measurement was determined in duplicate. The results are given in the table below.

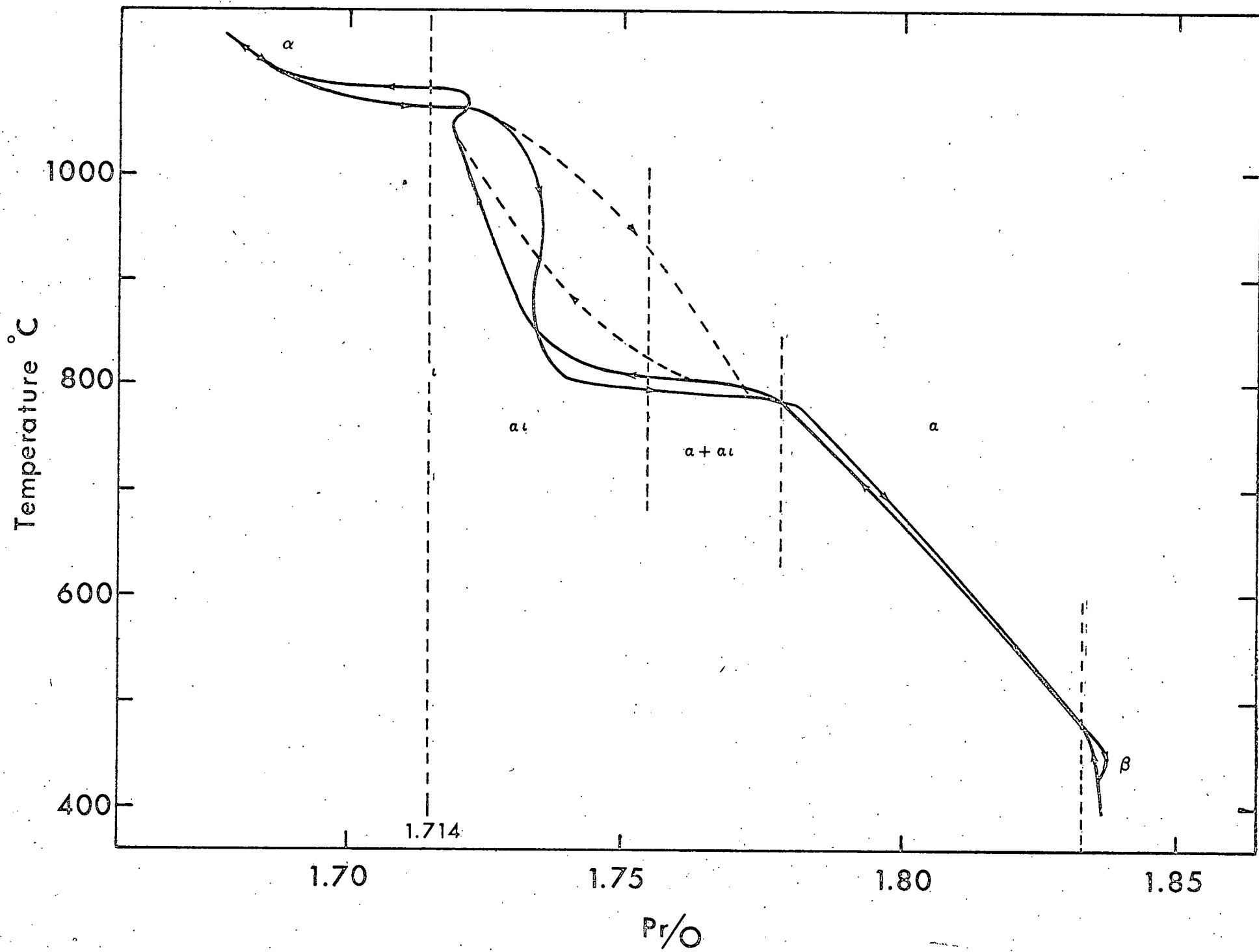
Run	Surface Area $M^2 \cdot g^{-1}$	Surface Area $M^2 \cdot g^{-1}$
1.	1.3	1.1
2.	0.94	0.97
3.	0.89	0.86
4.	0.91	0.87

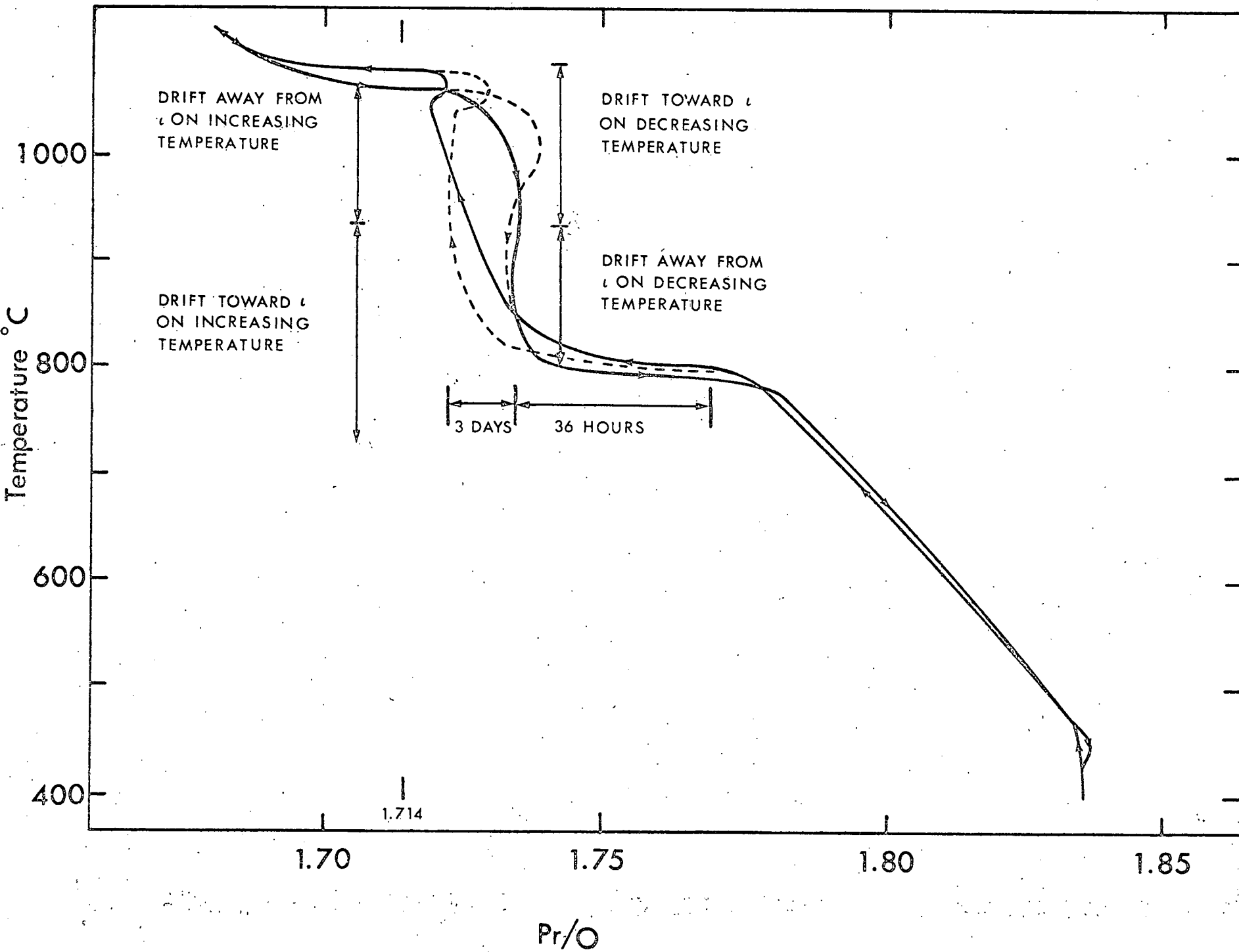
The initial decrease in surface area with increasing number of runs can be seen on comparing the surface area measured in Run 1 with the following measurements. The largest decrease in surface area is seen

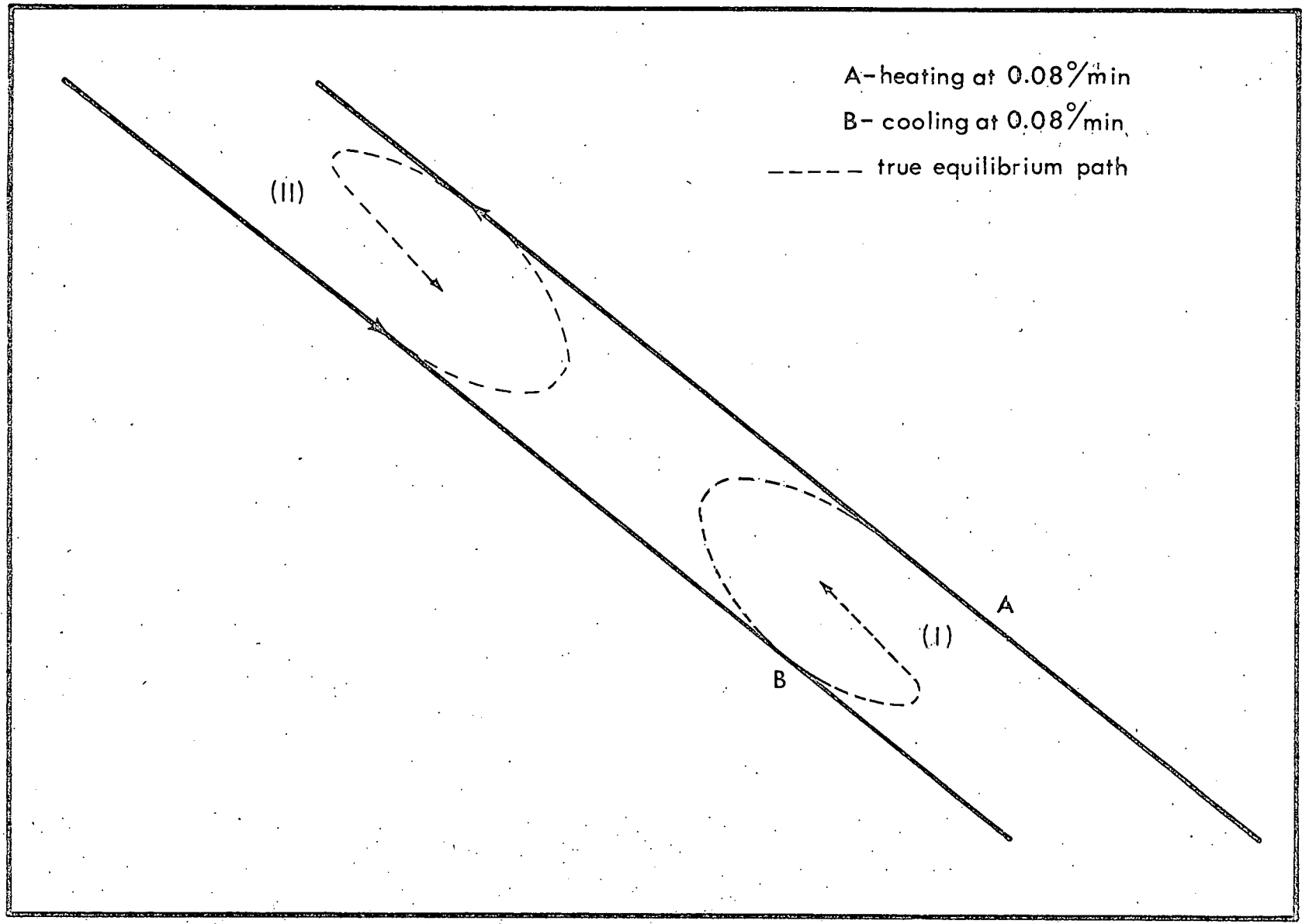
to occur after the first heating after which the surface area appeared to become constant. The surface area measurements are in good agreement with those measured by Schuldt¹⁰ on various praseodymium oxides, which he found to lie in the range 2.14 to 0.87 m².g⁻¹ and quantitatively show an initial decrease in surface area with increasing numbers of experiments.

REFERENCES

1. The Solid State Chemistry of Rare Earth Oxides--Technical Progress Report (1966-67) COO-1109-25.
2. Hyde, B. G., Bevan, D. J. M., and Eyring, L., Phil. Trans. Roy. Soc., A 259, 583 (1966).
3. Phillips, W. L., Trans. A.S.M., 57, 33 (1964).
4. Elliott, G. R. B., Lemons, J. F., Advances in Chemistry, 39, 153 (1963).
5. Roof, R. R., Elliott, G. R. B., Inorganic Chemistry, 4, 691 (1965).
6. Chikalla, T. D., Eyring, L., J. Inorg. and Nucl. Chem., 29, 2281 (1967).
7. Hagemark, H., Broli, M., J. Inorg. and Nucl. Chem., 28, 2837 (1966).
8. Everett, D. H., Nordon, P., Proc. Roy. Soc. A 259, 341 (1960).
9. Gallagher, K. J., Jenkins, M. S., J.C.S. (in press).
10. Schuldt, H. S., Ph.D. Thesis, University of Iowa, 1960.
11. Bevan, D. J. M., Kordis, J., J. Inorg. Nucl. Chem., 26, 1509 (1964).
12. Eyring, L., International Symposium on High Temperature Chemistry, Argonne National Laboratory, May 1967.







A- heating at 0.08%/min

B- cooling at 0.08%/min

----- true equilibrium path

(II)

(I)

A

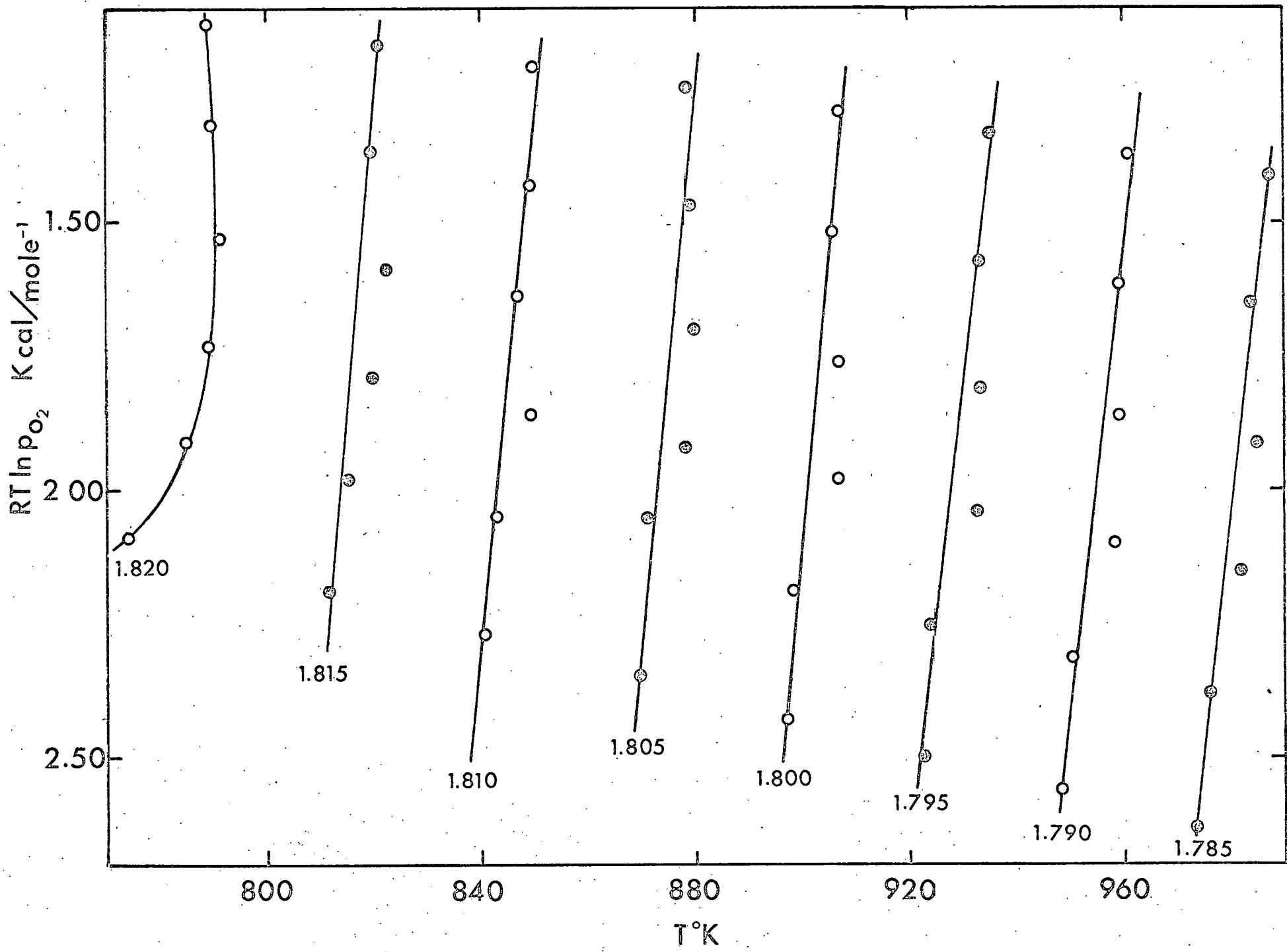
B

↑
Increasing Temperature

←

Loss in weight

Figure 3



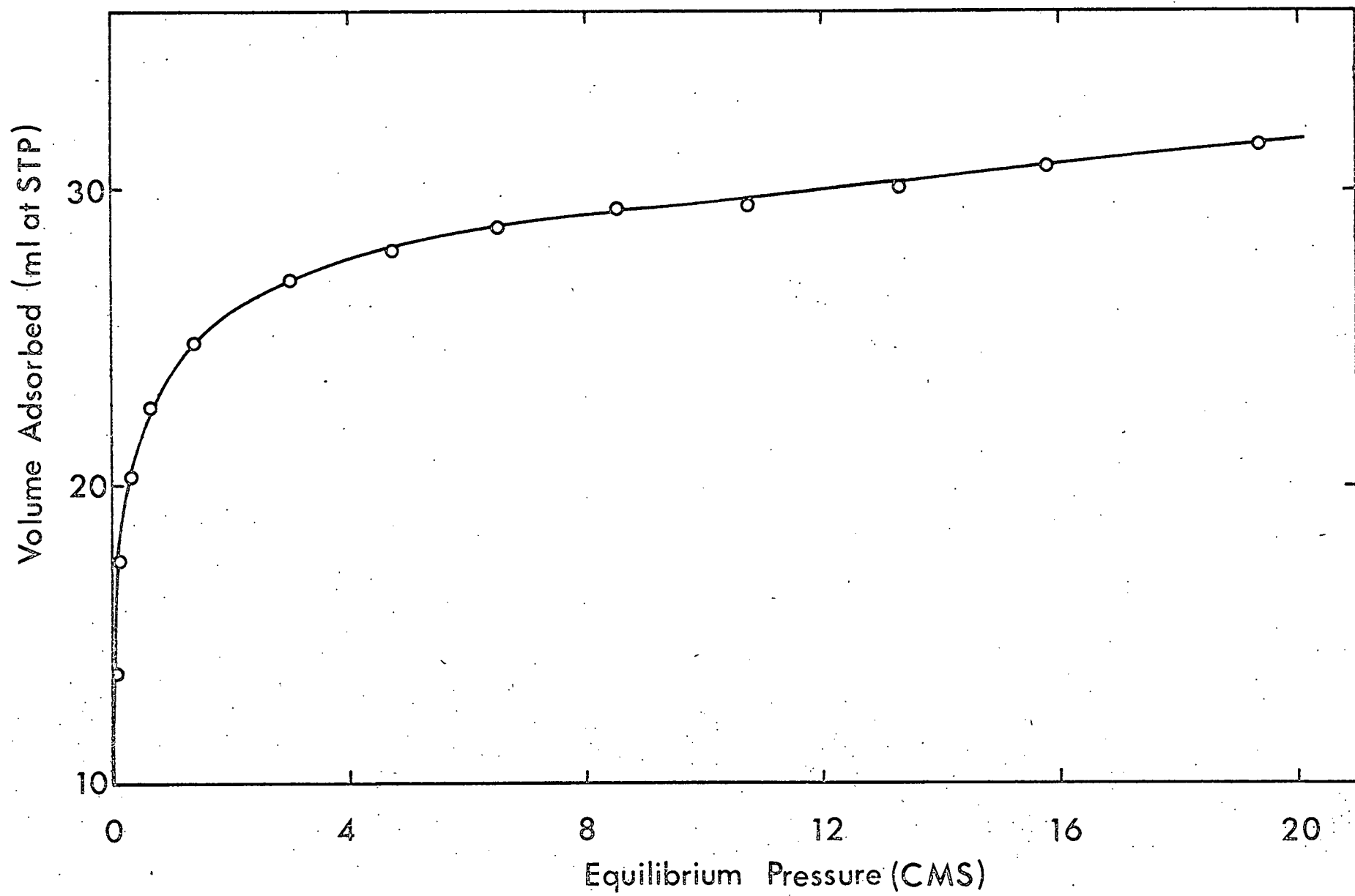


Figure 5

MASS TRANSPORT PROPERTIES

OF

RARE EARTH OXIDES

Theoretical Introduction

It is well known that Wagner and Schottky¹ were the first to show that at equilibrium a solid has a certain number of defects which are formed by the requirement that the free energy of the crystal be a minimum. These defects are the intrinsic defects formed without change in the overall composition of the crystal.

In Figure 1 a Frenkel defect is shown. It consists of an interstitial atom, that is one which is between the normal lattice sites, and a vacant lattice site. The number of Frenkel defects may be calculated as follows.

Let W be the work necessary to move an atom from a normal lattice site to a point far enough away so that there is no interaction between the two. Let N equal the total number of atoms in the crystal and αN the total number of interstitial sites. The number of ways that n interstitial atoms can be arranged on the αN interstitial sites is

$$P_i = \frac{(\alpha N)!}{(\alpha N - n)! n!} \quad (1)$$

For the number of ways the vacancies can be arranged on the lattice sites we have

$$P_l = \frac{N!}{(N - n)! n!} \quad (2)$$

The entropy is then

$$S = k[\ln P_l + \ln P_i]. \quad (3)$$

The increase in the internal energy of the crystal is

$$\Delta E = nW. \quad (4)$$

The requirement of thermal equilibrium gives the condition

$$\left(\frac{\partial F}{\partial n} \right)_T = 0. \quad (5)$$

Using stirlings approximation and applying the criteria above the number of defects n is

$$n = \sqrt{cN^2} e^{-\frac{1}{2}W/kT}. \quad (6)$$

As would be expected the intrinsic disorder of the crystal increases rapidly with increasing temperature and from the above equation the driving force for the formation of an interstitial is the increase in the configurational entropy with increasing number of defects. The same type of treatment can be given for Schottky defects.

In the more general case there is a vapor of one of the species in equilibrium with the crystal. By controlling the pressure of this vapor the composition of the crystal can be controlled. This gives rise to nonstoichiometry which was not considered above. The intrinsic defects predominate when the vapor pressure is such that the crystal is very nearly stoichiometric, the exact circumstances depending upon the substance under consideration.

The laws governing the concentration of defects present in a solid in equilibrium with the vapor of one of its components will now be derived. These laws will be given in the form of equilibrium constants using the laws of mass action. Thus for the reaction



the Frenkel constant can be written as

$$K_F = \frac{[O_i''] [V_O^{\bullet\bullet}]}{[V_i] [O_O^X]} = [O_i''] [V_O^{\bullet\bullet}] \quad (8)$$

where, using the notation of Kröger² V_i indicates a vacant interstitial site, O_O^x indicates an oxygen ion on an oxygen site, O_i'' indicates an oxygen ion on an interstitial site, and V_O^\bullet indicates a positively charged vacant oxygen site. The Frenkel constant may also be written in terms of the number of defects by eq (6), hence

$$K_F = [O_i''] [V_O^\bullet] = n^2 = cN^2 e^{-W/kT}. \quad (9)$$

Similarly the reaction for the formation of oxygen interstitials from oxygen gas can be written as



Assuming $[O_i''] = \frac{1}{2}[h^\bullet]$ the equilibrium constant may be written

$$K_1 = \frac{[O_i''] P^2}{P_{O_2}^{\frac{1}{2}}} = \frac{4[O_i'']^3}{P_{O_2}^{\frac{1}{2}}} = K_1' e^{-\Delta G_1/kT} \quad (11)$$

where ΔG_1 is the Gibbs free energy of formation of a doubly charged oxygen interstitial. If the assumption is made that this is the only type of defect, then the deviation from stoichiometry, x , is given by

$$x = [O_i''] = \left(\frac{1}{4} K_1' P_{O_2}^{\frac{1}{2}} \right)^{\frac{1}{3}} e^{-\Delta G_1/3RT} \quad (12)$$

or
$$x = K P_{O_2}^{\frac{1}{6}} e^{-\Delta G_1/3RT}. \quad (13)$$

In the general case x will be given by an expression such as

$$x = K P_{O_2}^{1/n} e^{-\Delta G/RT}; \quad (14)$$

the actual values of n and ΔG depend upon the material. The experimental values of these parameters should give some clue as to the defect present.

As the equation stands, the absolute value of the composition must be known to use the equation, however, in many instances it is not known exactly when stoichiometry is achieved. For these cases it is desirable to be able to use differences which can be measured fairly accurately. If the temperature is kept constant the deviation from

stoichiometry can be written as

$$x = c p_{O_2}^k. \quad (15)$$

Differentiating, one obtains

$$\frac{dx}{dp} = k c p_{O_2}^{(k-1)} \quad (16)$$

and taking the logarithm and substituting Δ 's for the d 's, equation (16) becomes

$$\ln \left(\frac{\Delta x}{\Delta p} \right) = \ln k c + (k-1) \ln p_{O_2}. \quad (17)$$

For a certain temperature the value of $k c$ will be a constant and a plot of $\ln \frac{\Delta x}{\Delta p}$ versus $\ln p_{O_2}$ will give the value of $k-1$ and hence k .

Alternatively the pressure can be kept constant and the temperature varied. Then, from eq (14) one has

$$x = c e^{-\Delta G/kt} = c e^{\Delta S/R} e^{-\Delta H/RT}, \quad (18)$$

or

$$\frac{dx}{dT} = \frac{C(\Delta H)}{kT^2} e^{\Delta S/R} e^{-\Delta H/RT}. \quad (19)$$

Again taking the logarithms of both sides the relation is

$$\ln \left(T^2 \frac{\Delta x}{\Delta T} \right) = \ln \frac{C(\Delta H)}{k} + \frac{\Delta S}{R} - \frac{\Delta H}{RT}. \quad (20)$$

A plot of $\ln \left(T^2 \frac{\Delta x}{\Delta T} \right)$ versus $1/T$ will yield a value for ΔH from the slope.

However, in doing this the assumption has been made that ΔG is constant over the temperature range. This is an approximation, since only if the entropy does not vary with temperature can a straight line be expected. Also the value of ΔH will depend upon the defect assumed to be present since in these plots the slope is equal to $-\frac{\Delta H}{nR}$ where n depends upon the defect present.

Diffusion

The solution of the diffusion equation for the uptake of solute from a well-stirred solution of limited volume has been given by Crank³ for the case when the mole fraction of solute in the gas and that in

the surface of the solid are assumed to be equal. The diffusion equation to be solved is

$$\frac{\partial c}{\partial t} = D \left(\frac{\partial^2 c}{\partial r^2} + \frac{2}{r} \frac{\partial c}{\partial r} \right) \quad (21)$$

with the initial condition

$$c = c_0, \quad a \leq r \leq 0, \quad \text{and } t = 0$$

which indicates that the concentration in the spheres at zero time is uniform. Also the amount of solute leaving the gas phase must equal that entering the solid, therefore,

$$V_g \frac{\partial c_g}{\partial t} = V_s D \left(\frac{\partial^2 c_s}{\partial r^2} + \frac{2}{r} \frac{\partial c_s}{\partial r} \right) \quad (22)$$

The solution is

$$\frac{M_t}{M_\infty} = 1 - \sum_{n=1}^{\infty} \frac{6\lambda(\lambda+1)\exp(-Dq_n^2 t/a^2)}{9 + 9\lambda + q_n^2 \lambda^2} \quad (23)$$

where the q_n 's are the non-zero roots of

$$\tan q_n = \frac{3q_n}{3 + \lambda q_n^2} \quad (24)$$

where M_t is the total amount of solute in the sphere at time t , M_∞ the total amount of solute in the sphere at infinite time, λ the ratio of the amount of oxygen in the gas to the amount in the solid, a the radius of the spheres, t the time, and D is the diffusion coefficient.

Computation

Tables of M_t/M_∞ versus Dt/a^2 were calculated using the GE 225 computer. These tables were calculated at intervals of one percent in terms of the fractional uptake. The determination of the diffusion coefficient then was made by calculating the values of M_t/M_∞ and the fractional uptake for a particular run. Then values of Dt/a^2 were obtained from the tables, and plots made of Dt/a^2 versus time. These plots are straight lines, the slopes being equal to D/a^2 .

A program was written to calculate the M_t/M_∞ values for the particular run. The system in which the experiments were run was divided into two volumes as noted in the reports of previous years. The calculations of M_t and M_∞ are easily made by the formulae

$$M_t = Vg(P_t - P_i) \quad (25)$$

and

$$M_\infty = Vg(P_f - P_i) \quad (26)$$

Their ratio is then

$$M_t/M_\infty = \frac{Vg(P_t - P_i)}{Vg(P_f - P_i)} = \frac{P_t - P_i}{P_f - P_i} \quad (27)$$

The fractional uptake then is given by the ratio

$$\frac{P_f - P_i}{P_s - P_i}$$

In these equations P_t is the percent of O^{18} in the gas a time t , P_i the percent of O^{18} in the gas at $t = 0$, P_f the percent of O^{18} in the gas at $t = \infty$, and P_s the percent of O^{18} in the solid at $t = 0$.

The computations involved in the weight measurements are straightforward. It is, however, worth demonstrating that the sample weight has no effect on the result if the change in weight instead of the change in y , the number of excess gram atoms of oxygen per mole of $PrO_{1.714}$ is used.

Let $AW_{1.5}$ equal the actual weight of $PrO_{1.5}$ and $MW_{1.5}$ equal the molecular weight of $PrO_{1.5}$ (the other subscripts follow) then

$$y = \frac{(AW_x - AW_{1.714})/16}{AW_{1.5}/MW_{1.5}} \quad (28)$$

or

$$y = \frac{(AW_x)(MW_{1.5})}{(16)(AW_{1.5})} - \frac{MW_{1.714}}{16} \quad (29)$$

The values actually measured are however Δy thus

$$\Delta y = \frac{(MW_{1.5})}{16(AW_{1.5})} \Delta(AW_x) = K\Delta(AW_x) \quad (30)$$

If the logarithm of both sides is taken

$$\log (\Delta y) = \ln K + \ln \Delta(AW_x) \quad (31)$$

it can be seen that the sample weight provides only an additive constant which will differ from run to run but will not change the slope of a plot of $-\log(\Delta y)$ versus $\ln \Delta(AW_x)$ where the changes will in fact of course be taken with respect to some variable such as temperature, pressure, etc. All calculations are, therefore, made in terms of the actual weight change rather than in terms of the change in y .

Experimental Results

The activation energy for the diffusion process was determined at two pressures, 30 mm, and 214 mm pressure of O_2 . The runs gave identical activation energies within the experimental error. The actual points are plotted in Figure 2 and the two lines can be represented by the two equations

$$D_{30} = 5.96 \times 10^{-6} \exp(-18.6 \pm 1/RT) \quad (32)$$

$$D_{214} = 1.19 \times 10^{-5} \exp(-18.9 \pm 1/RT) \quad (33)$$

The difference in the pre-exponential factors will be discussed later. The equation given for the run at 214 mm is only for the portion of the line which is straight. There is a break in the line at a value of $1000/T$ of approximately 0.915 and at lower temperatures the diffusion coefficient is almost constant as the temperature is raised. Table I lists the values of the diffusion coefficient and the temperature.

The pressure dependence of the diffusion coefficient at various temperatures is shown in Figure 2. The slopes of the lines give the pressure dependence. The values of the diffusion coefficient and the pressures are listed in Table II.

Table I

$$P = 29.4 \pm 0.1 \text{ mm}$$

D x 10 ⁹	T (°C)
0.733	735.0
0.684	752.7
0.777	771.7
0.970	799.2
1.16	839.0
1.39	845.5
1.62	865.9

$$P = 214.5 \pm 0.1 \text{ mm}$$

D x 10 ⁹	T (°C)
1.56	725.6
1.57	746.8
1.66	766.7
1.74	775.7
1.85	787.1
1.97	798.9
1.98	810.3
2.02	820.1
2.28	832.6
2.40	843.7
2.60	855.6
2.84	868.2
3.05	881.3
3.44	892.8
3.71	904.9
4.10	918.5
4.56	932.3

Table II

T = 734.6° C		T = 759.7	
D x 10 ¹⁰	P (mm)	D x 10 ¹⁰	P (mm)
5.03	11.21	4.57	10.50
5.57	13.93	5.52	20.83
5.48	17.65	6.70	33.01
6.36	22.41	7.72	50.04
6.29	28.01	8.91	74.25
6.50	35.08	10.3	103.88
7.17	44.80	12.4	139.16
7.42	55.59		
8.12	69.06		
8.26	87.23		
8.82	107.41		

T = 831°		T = 891.6	
D x 10 ⁹	P	D x 10 ⁹	P
1.23	18.61	2.78	21.03
1.29	25.53	2.67	27.51
1.41	34.04	2.67	36.27
1.39	44.41	2.48	48.78
1.46	57.59	2.50	62.55
1.68	75.31	2.54	82.38
1.77	95.30	2.63	107.93
1.89	123.90	2.95	140.15
2.08	162.56	3.26	191.19

Thermogravimetric analysis runs were made at both constant temperature and constant pressure. In Figure 3 the results of a run at constant temperature are plotted. The change in weight is proportional to the square root of the pressure. This was true in all four of the runs made, within the experimental error. However, it is to be noted that the temperature range investigated so far has been extremely limited. The temperatures ranged from 720 to 764°. The values of the slope and the temperatures are listed in Table III. The runs were made on samples of approximately 7 grams. The total weight change was about three milligrams in the pressure region 10-200 mm. Buoyancy becomes a large effect when working with weight changes of this order of magnitude. Figure 4 shows a graph of the correction determined by using nitrogen. Below 10 mm pressure the buoyancy correction becomes much larger than the weight changes and, therefore, data for pressures less than 10 mm have not been used. The reason for the large buoyancy correction is probably thermomolecular flow which is expected to become important in this pressure region. A way around this is, of course, to use an inert gas-oxygen mixture instead of pure oxygen. However, the design of the apparatus at present makes such experiments impractical. The buoyancy corrections in nitrogen were multiplied by $32/28$ to obtain the approximate correction in oxygen.

Isobaric TGA runs were also made. One at 10 mm oxygen pressure is shown in Figure 5 and one at 214 mm in Figure 6. These runs were made by increasing the temperature by 0.8°/min. The temperature of the weighing was determined from the automatic pen on the chart. For the run at 214 mm the weight readings were taken at equal time intervals. The temperature change of the furnace is programmed to be as near linear

Table III

T °C	slope
721°	0.55
726.5°	0.50
746°	0.50
764°	0.53

as possible. It appeared to be linear over the temperature range of interest when a ruler was placed next to the recorded trace. Therefore, instead of actually reading the temperature of each point the two end-point temperatures were read and the temperatures of the intervening points were determined by interpolation. This was justified since the change was programmed to be linear and this technique would smooth the trace on the graph which consisted of small jumps in temperature which are not possible in reality because of the thermal inertia of the furnace. Thus the points in Figure 6 appear to form two regions which approximate straight lines yielding two energies of formation (Figure 6); -37.4 kcal and -12 kcal. In Figure 5 only one energy is indicated (-10.4 kcal). It is not possible to accurately estimate the error in these measurements, we are interested more at this point in their qualitative values.

An isobaric run at 195 mm pressure is shown in Figure 7. This run was made at a slower speed, 0.45°/min and the temperature was measured for each point by using a potentiometer instead of the automatic recorder. It is debatable whether the graph shows two regions as in Figure 6 or only one. If it shows two, they are not as well separated as in Figure 6 and the energies are different. If only one line is drawn, the value is about -20 kcal.

The values of the enthalpies given above are calculated on the basis that the slope is equal to $\Delta H/R$ and hence must be multiplied by a suitable factor if the actual defect assumed to be present would give a slope equal to $\Delta H/2R$ or $\Delta H/3R$.

Discussion

In order to judge between possible diffusion mechanisms it is necessary to determine from gravimetric analysis whether the compound

exists in a hyperstoichiometric or a hypostoichiometric condition in the range of temperatures and pressures that the diffusion coefficient is to be measured. The gravimetric studies of the praseodymium oxygen system indicate, within the experimental error, that the $\text{Pr}_7\text{O}_{12+\delta}$ phase over its range of existence is either hyperstoichiometric or stoichiometric, but never hypostoichiometric. When the temperature is increased to where one would expect the compound to be oxygen deficient it becomes unstable and decomposes.

With these facts in mind two possibilities must be considered for the deviation from stoichiometry. One, oxygen may be taken up according to the reaction



(that is, the oxygen may go into empty oxygen lattice sites on the surface of the crystal with the simultaneous formation of praseodymium vacancies). Alternatively, the excess oxygen could be accommodated in the lattice by occupying empty interstitial oxygen sites in the compound as represented by the reaction



Unfortunately, X-ray diffraction studies of the phase over its range of composition show that within experimental error the lattice parameter is constant. Therefore, indirect means must be used to differentiate between these two possibilities.

The structure of the intermediate praseodymium oxides have not been discussed here, but let it suffice to say that they are derived from the fluorite type lattice of PrO_2 by removing oxygen in an ordered way to form the composition desired. Although the intermediate phases have lower symmetry than the parent dioxide, the metal lattice is only

slightly distorted and the metal positions shift, only slightly.

The $\text{PrO}_{1.714}$ phase has a rhombohedral unit cell with angles of $99^\circ 23'$ and $a = 6.750 \text{ \AA}$. It may be considered as consisting of strings of oxygen vacancies at regular intervals all in the $\langle 111 \rangle$ direction of the parent fluorite unit cell. This indicates that it is more likely that the excess oxygen atoms occupy interstitial sites rather than generating cation vacancies since the cations appear to be the backbone of the structure. The fact that sintering of these materials requires high temperatures is also in accord with low cation mobility. The diffusion data support a model based upon interstitial oxygen since D_o increases with increasing pressure of oxygen indicating a positive pressure dependence for the diffusion coefficient. Thus in the ensuing discussion it will be assumed that equation (35) correctly describes the incorporation of oxygen into the structure.

Equation (35), however, besides indicating that the excess oxygen is interstitial in nature, also indicates that it is uncharged. Two points about reaction (35) have to be decided. Is the oxygen charged and, if so, what is the charge; also, is the interstitial site one of the "vacancies" formed by removing an oxygen from PrO_2 , or is it any of a number of other interstitial positions in the structure?

The question of where these interstitials are located in the structure cannot be answered unambiguously since there is no direct experimental evidence on this point. But in view of the fact that the compounds are formed by removing oxygens from a fixed network of cations, it seems logical that these are the spaces filled as the compound oxidizes. If a calculation is made of the size of the "vacancy" in $\text{PrO}_{1.714}$, assuming the structure to be isomorphous with U_6O_{12} , the "vacancy" is larger than

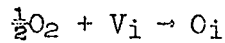
the other holes in the structure, having a diameter of 2.23 Å. This is large enough to easily accommodate an oxygen atom or singly charged oxygen, but a little small for a doubly charged oxygen having a radius of 1.4 Å. Although it has been proven that the metal positions in these two compounds are identical, the oxygen positions may be slightly different, due to the fact that the electrostatic interactions of the two compounds with the oxygen atoms will be quite different. The UY_6O_{12} is composed of hexavalent and trivalent cations, while Pr_7O_{12} contains trivalent and quadrovalent cations. The X-ray technique used for the structure determinations is not particularly sensitive to the position of light atoms in a heavy atom matrix. Thus, the calculation of the size of the interstitial hole may be in error. The cell parameters and the interaxial angle for the two compounds based upon the rhombohedral cell are

	a.	α
UY_6O_{12} ⁴	6.530	99° 3'
Pr_7O_{12} ⁵	6.750	99° 23'

Consider now the portions of the curves in Figure 2, which have an activation energy of 18.7 kcal. An attempt will be made to show that, as far as the data collected up to this point are concerned, this portion of the curves can be explained on the basis of there being one type of defect for the particular pressure and temperature range over which the curves are linear.

One of the primary reasons for making this assumption is that the activation energy for the diffusion process is the same at both pressures. In addition, though, the enthalpy of formation of the defect in these regions as determined from the TGA work seems to indicate the same energy of formation for the defect, approximately

-11 kcal. If this is taken as a fact, even though the TGA data are not conclusive on this point, the next question is the pressure dependence of the diffusion coefficient. The pressure dependence was measured and found to be $\frac{1}{4}$ (see Figure 8). Consider the reaction for the incorporation of oxygen gas into the solid to form neutral interstitial oxygen atoms



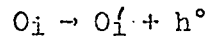
with
$$K_1 = [O_i] p_{O_2}^{\frac{1}{2}}$$

or solving for the concentration of interstitial oxygen atoms

$$[O_i] = K_1 p_{O_2}^{\frac{1}{2}}. \quad (36)$$

The concentration of interstitial oxygen atoms would change with the square root of the oxygen pressure, thus it can be ruled out as the defect.

The interstitial atom could pick up an electron to form a negatively charged oxygen according to the reaction



which yields

$$K_2 = \frac{[O_i']P}{[O_i]}$$

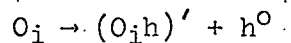
Setting $[O_i'] = P$ the equation becomes

$$[O_i']^2 = K_1 K_2 p_{O_2}^{\frac{1}{2}}$$

and the pressure dependence of the defects is

$$[O_i'] = \sqrt{K_1 K_2} p_{O_2}^{\frac{1}{4}}. \quad (37)$$

Another defect reaction which may be postulated is



yielding

$$K_3 = \frac{[(O_{ih})']P}{[O_i]}$$

for which the pressure dependence is

$$[(O_{ih})'] = \sqrt{K_1 K_3} p_{O_2}^{\frac{1}{4}}. \quad (38)$$

In these equations two species having a pressure dependence of one-quarter have been postulated. The first defect is a singly charged oxygen ion and a dissociated hole; the second consists of an associated, doubly charged oxygen and hole, plus a dissociated hole. These are not both in the solid at the same time, for if they were, the concentration of the particular defect could not have been set equal to the concentration of the positive hole.

The difference between the two types of defects is subtle; that is, both consist of two parts--a hole and a negatively charged species. However, in one case the negative charge consists of two associated species, while in the other the negative charge is a simple species. With the information at hand a choice between these two defects cannot be made.

In the discussion thus far, it has been assumed that the activity coefficients for all the species are one, a fact unverified experimentally and perhaps open to serious question since the holes are formed by the reaction



and the holes are the Pr^{+4} ions. The compound already contains a large number of plus-four ions. It is assumed, however, that since the compound is relatively stable, it has a unique electronic structure and that when this is disturbed by adding holes, the activity coefficients are nearly one.

Assuming the defect to be one of the two types considered and hence consistent with the data at present, the energetics of the diffusion process can be examined. In its simplest formulation the diffusion coefficients can be written as

$$D = D_i F_i \quad (40)$$

where D is the measured diffusion coefficient, D_i is the intrinsic diffusion coefficient, or the diffusion coefficient of a defect. The term F_i is the atom fraction of the defects. This latter term is purely a thermodynamic term and is given by the expression.

$$F_i \propto e^{-\Delta G_f^\circ/RT} = e^{\Delta S_f^\circ/R} e^{-\Delta H_f^\circ/RT}$$

where ΔG° , ΔH° and ΔS° are respectively the Gibb's free energy, enthalpy and entropy of formation of the defects. For the species proposed above, the equilibrium constant can be written

$$\frac{[(O_{ih})'] P}{K_1 P_{O_2}^{1/4}} = B^2 e^{-\Delta H^\circ/RT}$$

and setting $[(O_{ih})] = P$ and solving for $[(O_{ih})']$ the temperature and dependence is

$$[(O_{ih})'] = BK_1' P_{O_2}^{1/4} e^{-\Delta H^\circ/2RT}. \quad (41)$$

Substituting this into the equation for D , the result is

$$D = D_i BK_1' P_{O_2}^{1/4} e^{-\Delta H^\circ/2RT}. \quad (42)$$

This expression indicates that the diffusion coefficient should be proportional to the fourth root of the pressure, a result which was put into the model through the choice of the defect. It also indicates that

$$\left(\frac{\partial \ln D}{\partial (1/T)} \right)_{P_{O_2}} = \frac{\partial \ln D_i}{\partial (1/T)} - \frac{\Delta H_f^\circ}{2R} = -\frac{\Delta H_m}{R} - \frac{\Delta H_f^\circ}{2R} = -\frac{\Delta H_{act}}{R}$$

or

$$\Delta H_{act} = \Delta H_m + \Delta H_f/2. \quad (43)$$

This equation arises because the number of defects at constant pressure of oxygen changes as the temperature is changed. The entropy terms in the expressions above have been assumed to be independent of temperature.

The information known is enough to estimate ΔH_m . The activation energy is known from the temperature dependence of the diffusion

coefficient and the enthalpy of formation of the interstitials has been estimated from the TGA runs. We have values of both -40 and -22 kcal for the enthalpy of formation. These values give respectively 8.7 and 13.2 kcal for the enthalpy of motion. At this time, it is not possible to say which value is correct. Further experiments will be necessary to decide.

In accordance with the fact that the diffusion coefficient is dependent on the fourth root of the oxygen pressure, the pre-exponential terms in the expression for the diffusion coefficients at 30 and 214 mm pressure should be in this ratio. The ratio may be expressed as

$$\frac{D_{O_1}}{D_{O_2}} = \frac{p_1^n}{p_2^n}$$

and solving for n

$$n = \log (D_{O_1}/D_{O_2}) / \log (p_1/p_2)$$

and substituting the experimental values of the parameters the result is

$$n = \log (2.0) / \log (7.14) = \frac{0.3}{0.854} = 0.35. \quad (44)$$

Although n is not equal to 0.25, the agreement is considered satisfactory since the range over which the diffusion coefficient was measured was limited and the extrapolation required to obtain D_0 was quite long. The expression for the diffusion coefficient can now be written

$$D = 2.84 \times 10^{-6} p_{O_2}^{\frac{1}{4}} e^{-(18.7 \pm 1)/RT} \quad (45)$$

where the pre-exponential factor is the average of the values calculated at the different pressures.

Until the discrepancy in the TGA work is resolved, there is probably very little value in trying to analyze the curves further as far as specific mechanisms and defects are concerned.

The diffusion data, however, do seem to be consistent to the extent that both the isobaric and isothermal diffusion runs indicate a break in their behavior at 820° (see Figures 2 and 6). The large pressure dependence of 0.38 at 760° is in agreement with the discontinuity observed in the activation energy run at 214 mm pressure.

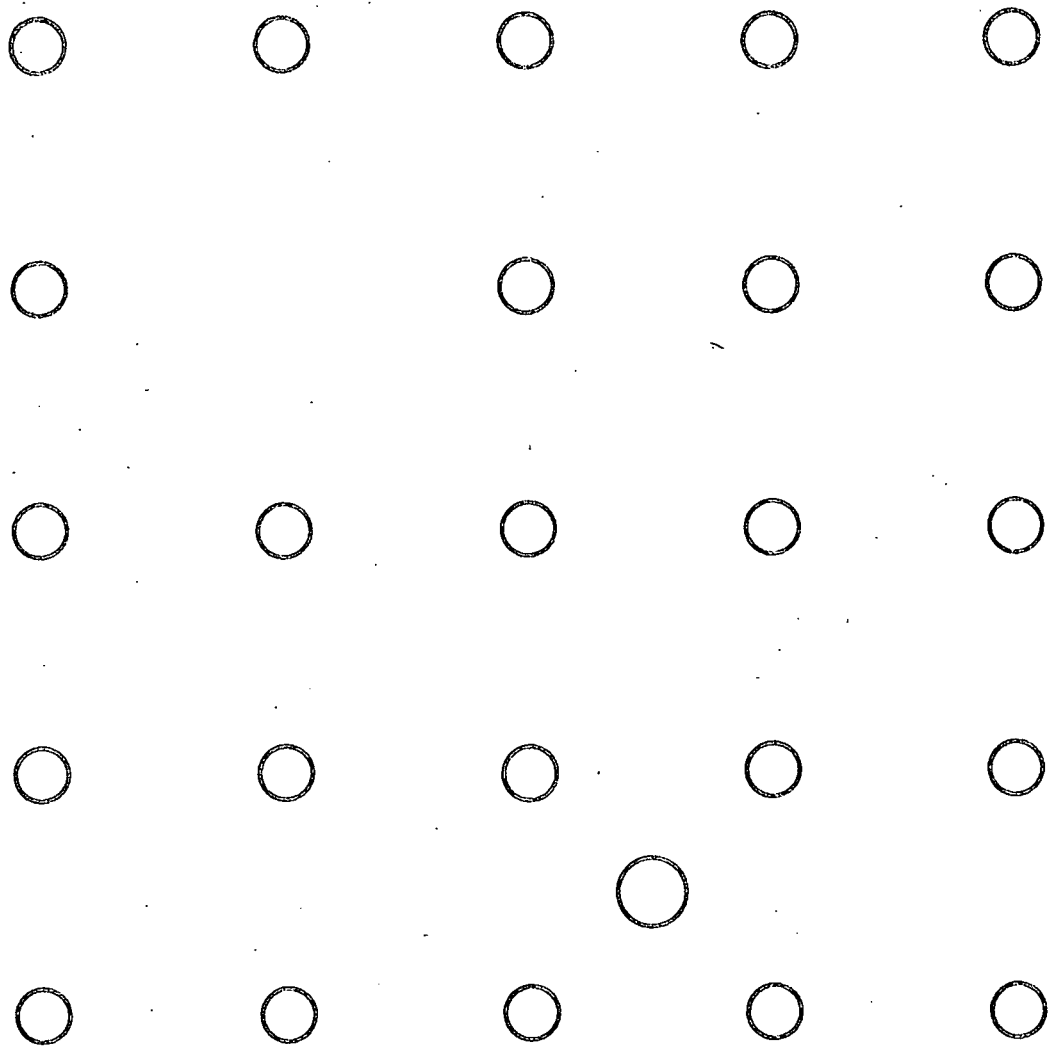
It should be pointed out the absolute value of the diffusion coefficients given here could be in error by an order of magnitude and should be considered as an upper limit to the real value. There are a number of reasons for this: 1) the radius of the spheres used for the calculation of the diffusion coefficient was that obtained from the average of the sieve sizes used for separating the spheres, 2) the sample is definitely polycrystalline and therefore contains grain boundaries, and 3) there is difficulty in obtaining whole spheres which are not slightly broken because of the phase transformation which must be made in these preparations.

It is believed, however, that the sample has not changed significantly during the course of the run and, therefore, that the relative values of the diffusion coefficients are correct.

The relationship between the pressure dependence and the diffusion coefficient and of the excess oxygen in $\text{PrO}_{1.714}$ has not been discussed. In the simplest case the pressure dependence of the two should be equal; however, in the measurements made thus far, they are not. The reasons for this are not known, and the measurements will not be discussed until they are more firmly established.

REFERENCES

1. Wagner, C., and Schottky, W., Z. Physik. Chem., B11, 163 (1931).
2. Kröger, F. A., The Chemistry of Imperfect Crystals, Amsterdam, North Holland Pub. Co., New York, Interscience Publishers, 1964, p 996.
3. Crank, J., Mathematics of Diffusion, Clarendon Press, Oxford, 1956, p 88.
4. Bartram, S. F., Inorg. Chem., 5, 749 (1966).
5. Eyring, L., and Baenziger, N. C., J. Appl. Phys., Suppl. 33, 428 (1962).



FRENKEL DEFECT

Figure 1

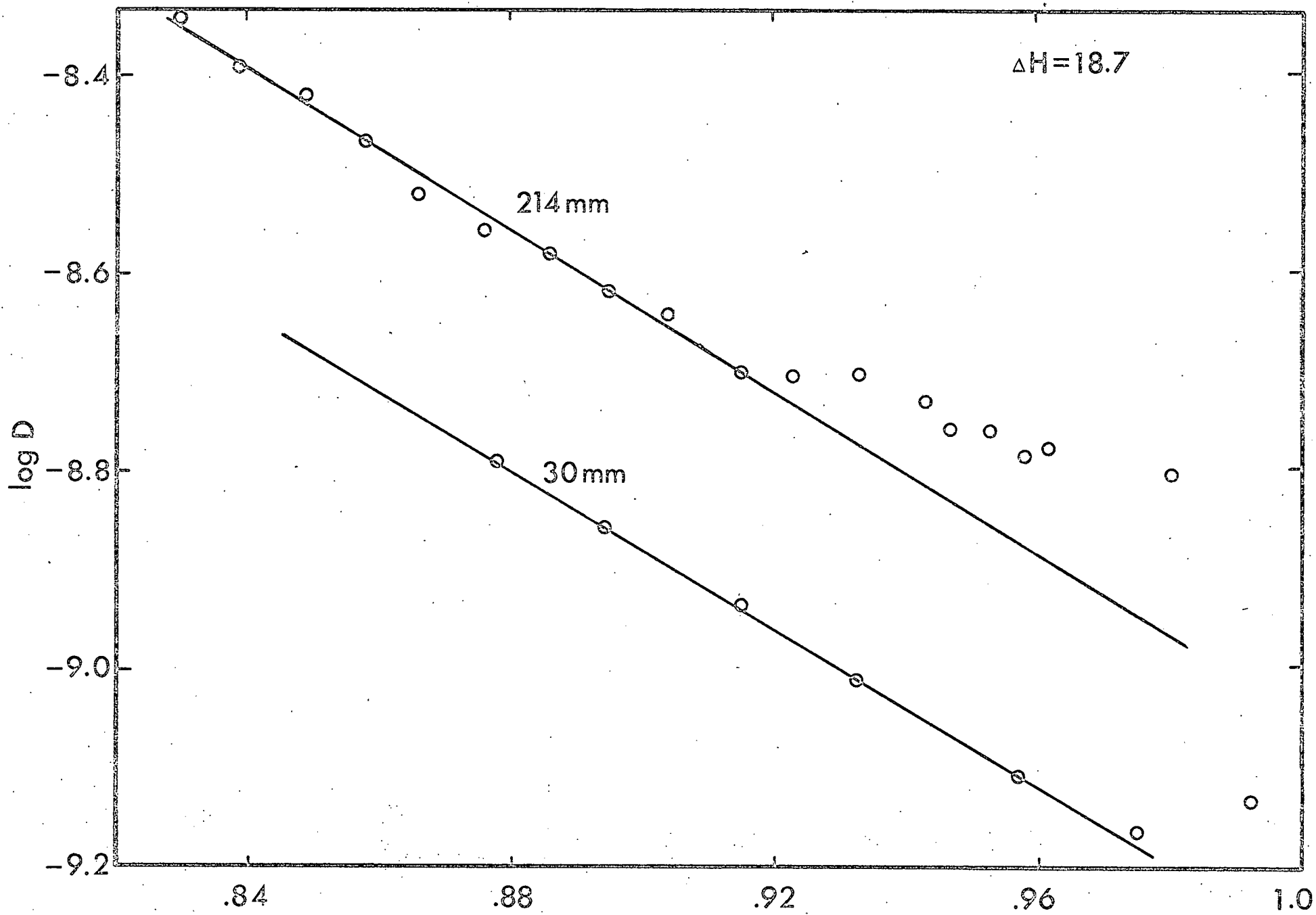


Figure 2

$\frac{1000}{T}$

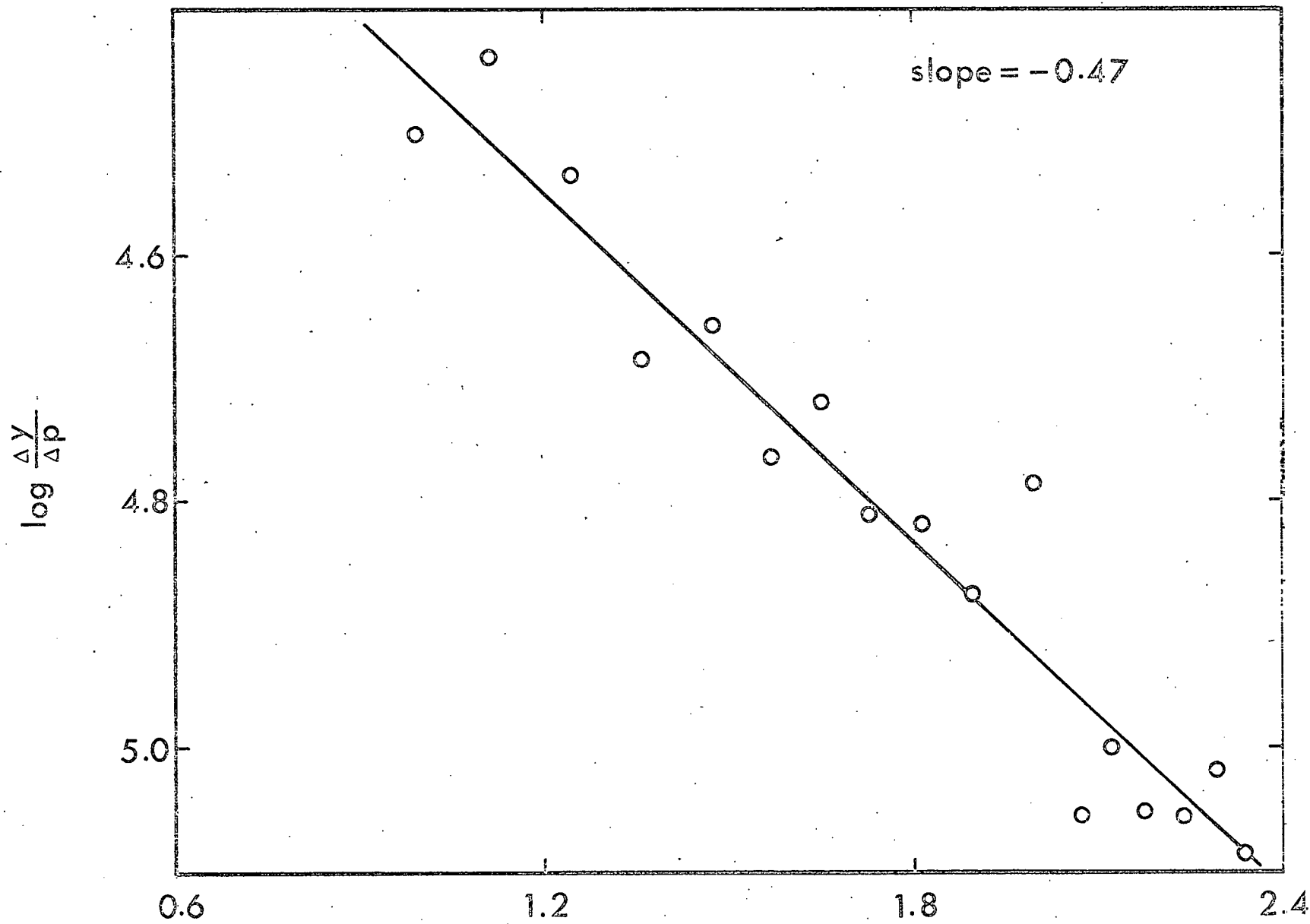
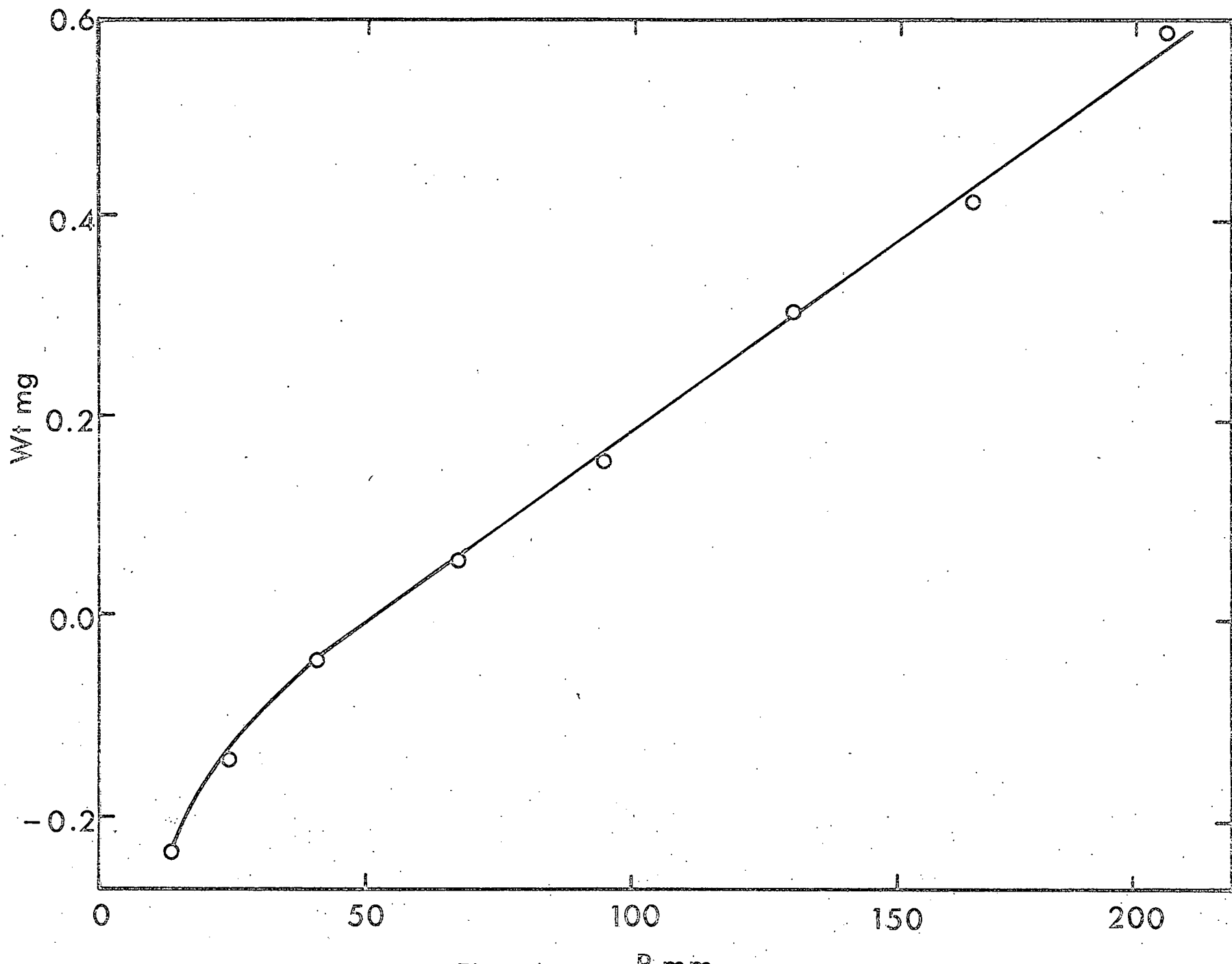


Figure 3 $\log P$



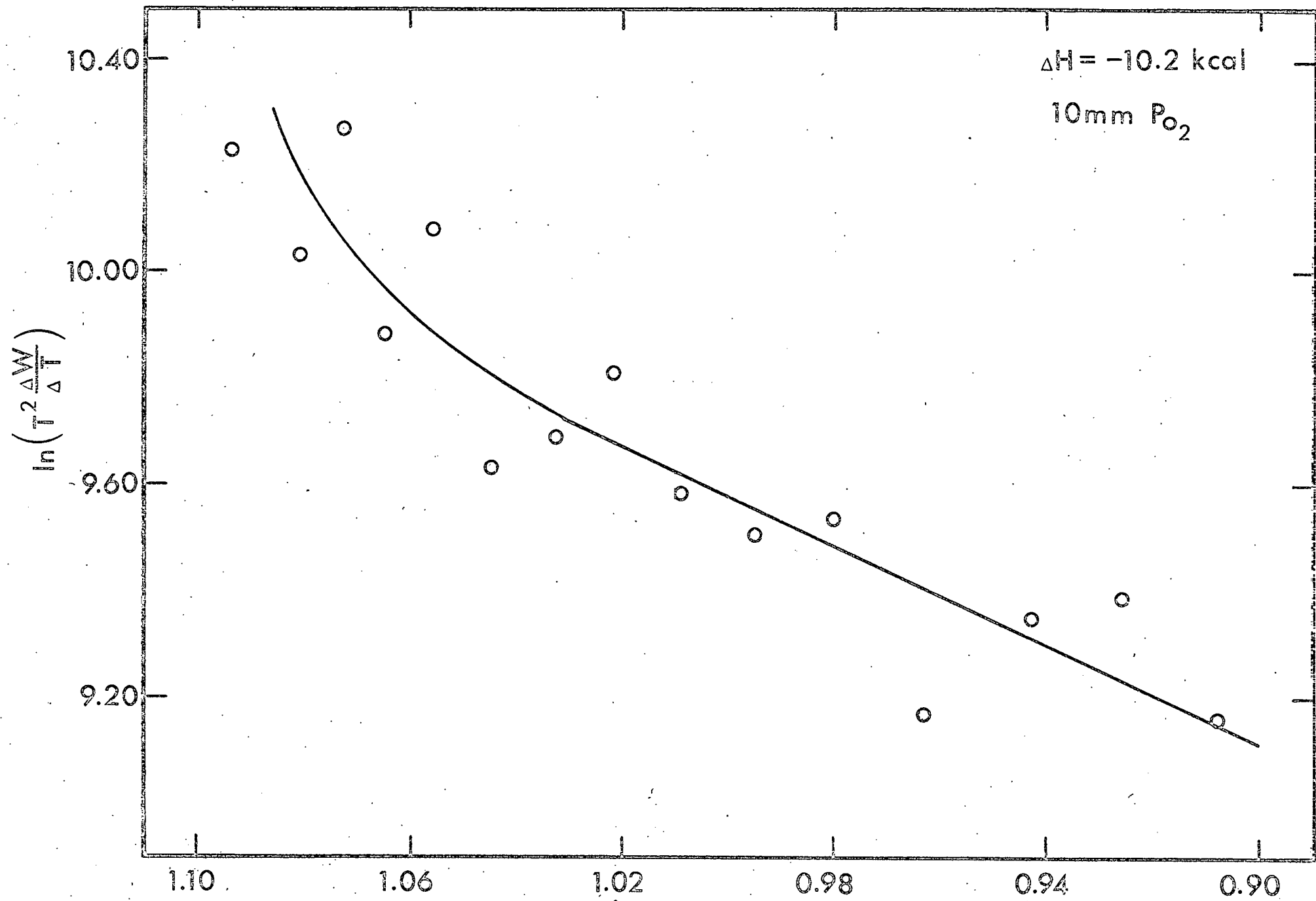


Figure 5 $\frac{1000}{T}$

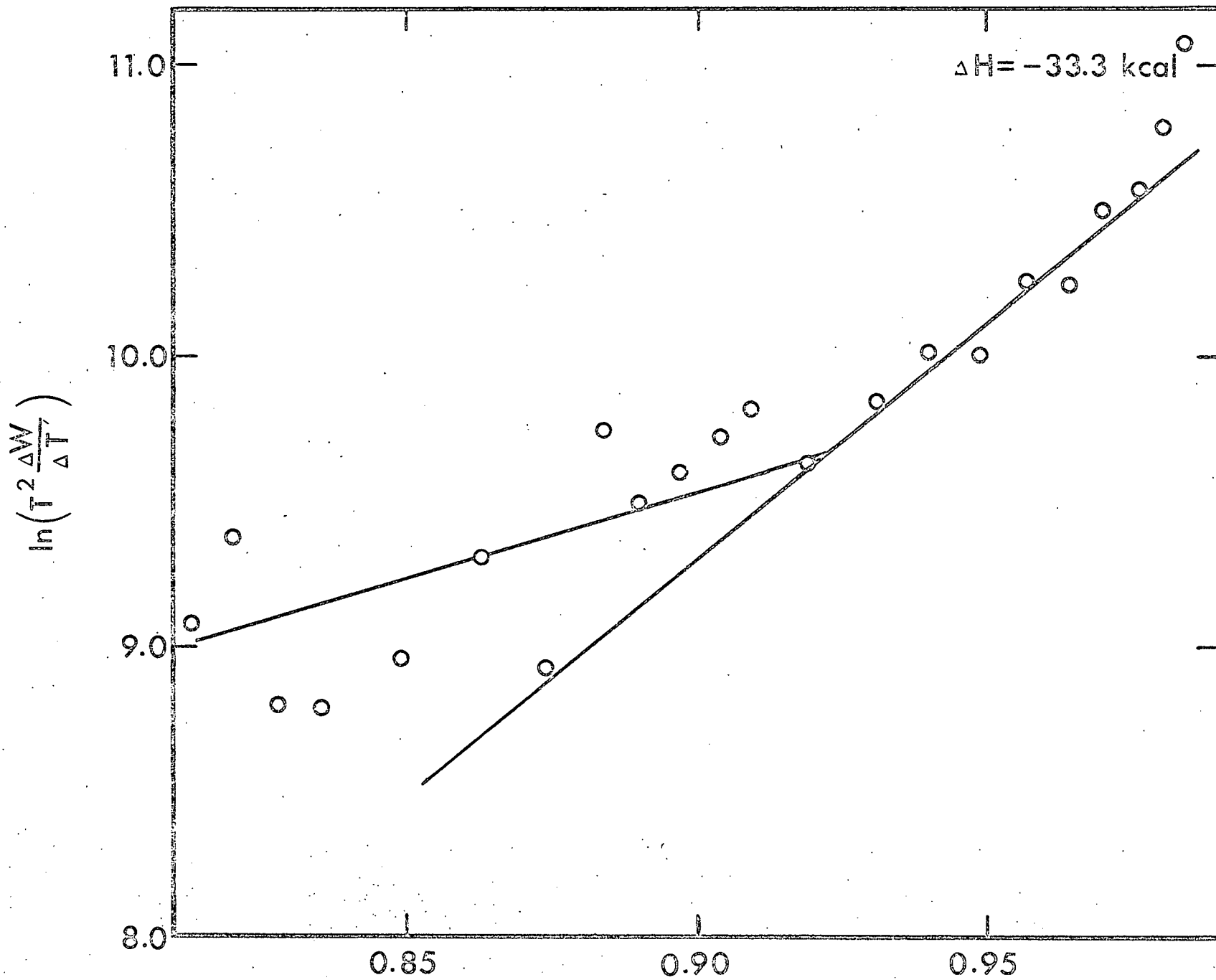


Figure 6 $\frac{1000}{T}$

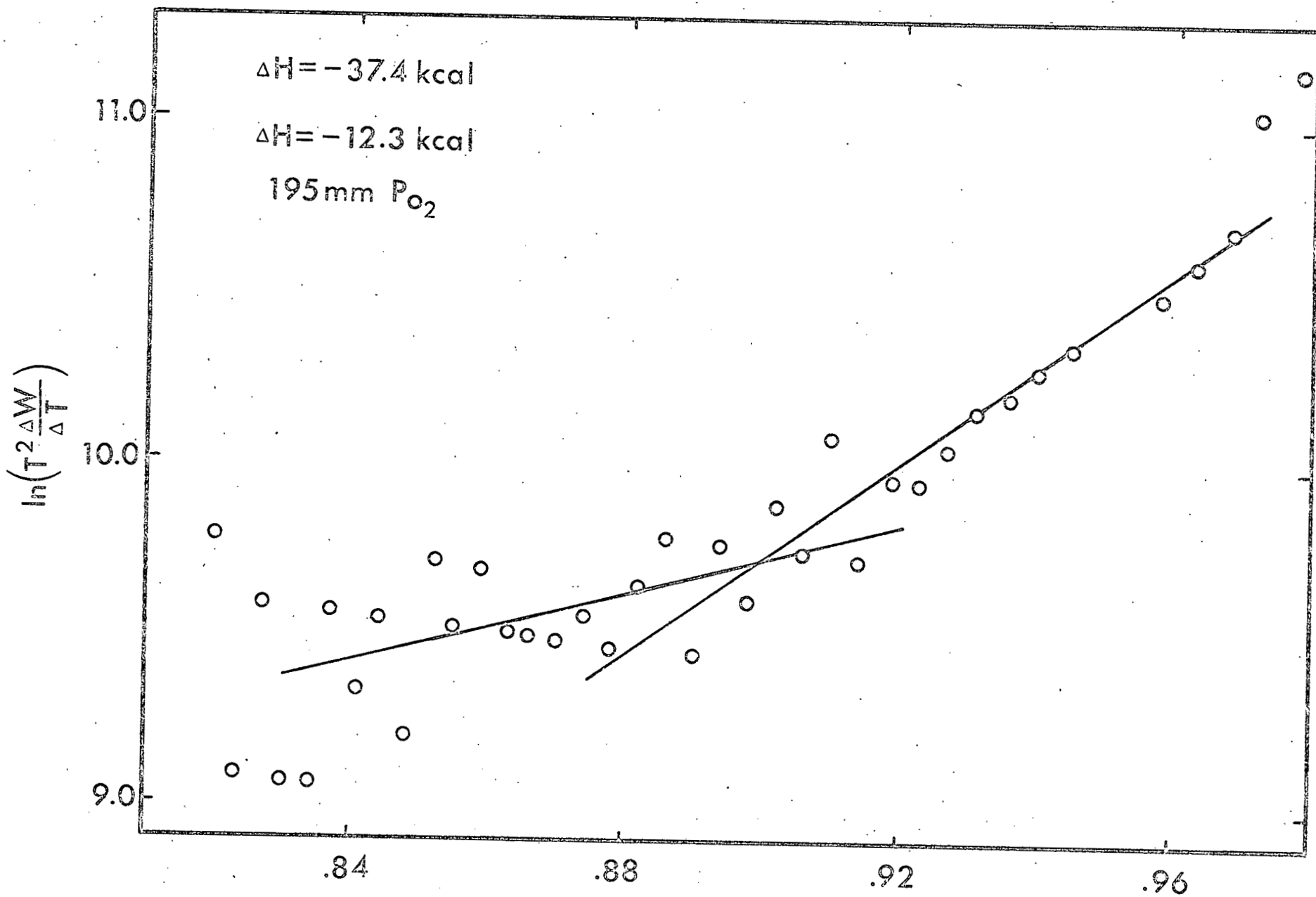
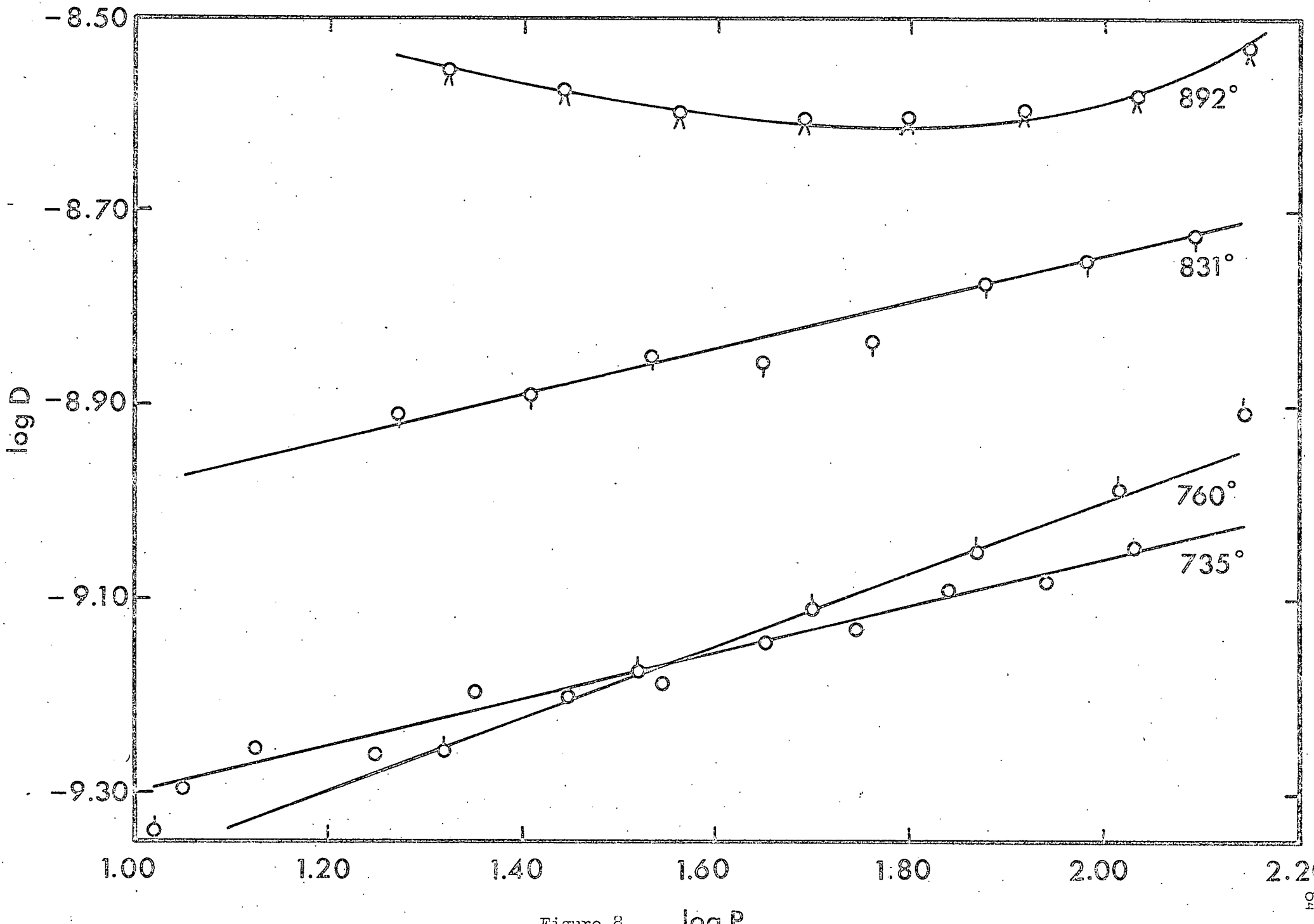


Figure 7 1000



HIGH TEMPERATURE X-RAY DIFFRACTION STUDIES

Introduction

The pseudophase regions in the $\text{PrO}_x\text{-O}_2$ system remain a primary interest as these are perhaps the least well understood areas. It is hoped that the study will give information concerning the role of disorder-order transformations in these regions. The microdomain concept which seems to be the most reasonable explanation of much of the nonclassical behavior experienced needs to be rigorously examined in the light of X-ray evidence. The Guinier high temperature camera is now in use and will give the most detailed information possibly attainable by powder methods. The diffractometer study reported here has yielded some useful information concerning the α_z region but the interpretations made can be regarded only as tentative due to the lack of complete detailed data.

The High Temperature Diffractometer System

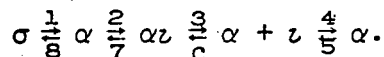
The diffractometer system has been modified in certain respects since last described (see previous reports for a complete description of the apparatus). The intensity of a given reflection has been doubled by installation of a broad focus copper tube while resolution appears to be little affected. Unfortunately superlattice reflections of the ordered phases remain undetectable but the improved intensity in the high angle region allows more accurate lattice parameter determinations.

In order to extend maximum temperatures attainable at one atmosphere pressure, a second auxiliary furnace was installed in the chamber. This Pt-10% Rh winding (alumina support) remains in the chamber when the main furnace and sample are removed. Power feed through is via a Conax gland which is tapped into the optical view port. The auxiliary furnace is controlled with a small variac. The maximum temperature now attainable at 730 mm O₂ pressure is 1160°

In order to eliminate the stepped temperature changes and the constant attention previously required when making a run, the 22 ampere Powerstat which controls the main furnace has been coupled to a variable drive DC motor by two 150:1 gear reducers. The design allows use of one or both reducers giving automatic increase or decrease in temperature at rates varying between 1000°/hr and 10°/hr.

The High Temperature Region in the PrO_x-O₂ System

The composition region PrO_{1.68} - PrO_{1.74} has been extensively investigated by the thermogravimetric technique.¹ At low pressures phase changes approach classical behavior. At higher O₂ pressures (P > 500 mm) the curves shown in Figure 1 have been interpreted in terms of the following transformations:



Transformations 1 and 7 are seen to be more complete and the pseudophase αz (so called due to its reproducible bivariant character) shifts to higher composition the higher the pressure. A previous investigation² of this area with the diffractometer did not yield X-ray evidence for the proposed phase changes. For this reason a more detailed study was made at several pressures.

Experimental Part.--Praseodymium oxide of 99.999% purity (with respect to rare earth) and supplied by the American Potash and Chemical Corporation was applied to 0.030" alumina slides via a toluene slurry and mounted in the high temperature chamber. Runs 36, 37, 38, 39 were made with the same sample. Runs 41 and 42 were made with two new samples. In all cases a pretreatment of several hours pumping at $\sim 600^\circ$ was carried out insituo. Although in many cases complete scans were taken the pertinent information is best gleaned from an examination of the pseudofluorite (200) reflection. Traces of this peak as a function of temperature are shown in Figures 2, 3, 4, 5, 6, 7, and 8.

Heating at 730 mm O₂ Pressure, Run 36.--As shown in Figure 2, at 746° only pure alpha is seen, but by 867° there is approximately 30% α . At 987° there are clearly three peaks, with the alpha peak in the center but shifted toward the $\alpha\alpha$ ($\bar{2}20$) (higher 20). Relative intensities as estimated with the DuPont curve resolver indicated that 38% alpha still remained. At 1057° the (220) α reflect on appears to be shifted toward the (220) $\alpha\alpha$ peak indicating reduction of the alpha phase. There does not seem to be a change in relative amounts of the two phases. It is noteworthy that although the (220) α peak overlaps the (220) $\alpha\alpha$ peak more than it does the ($\bar{2}20$) $\alpha\alpha$, the latter appears to be more intense. This same observation is made in other experiments and is a reproducible phenomena. The next scan taken at 1123° shows only the σ phase.

Cooling at 500 mm O₂ Pressure, Run 37.--At the conclusion of Run 36, the pressure was lowered to 500 mm and the cooling cycle begun. At the maximum temperature a broad low intensity peak appeared on the low angle side of the (440) σ (pseudofluorite (220)) reflection which

persisted at lower temperatures. This is apparently the result of a partial reaction most probably with the alumina slide on which the sample rests. There are further indications from the tensimetric work that reaction with alumina does take place to a small extent at elevated temperatures. The reflection at 1083° shows splitting, which is not characteristic of $\alpha_1 \alpha_2$ resolution. Although not shown, the (311) reflection shows even more clearly the growth of a second phase having a smaller lattice parameter and therefore more oxidized than the σ phase. The growth is not typical of ν growing in σ (Run 42) but appears to be $\sigma \rightarrow \alpha$. The next scan at 1031° shows 75% conversion to $\alpha\nu$ with the (220) α peak nearly entered between the $(\bar{2}20) - (220) \alpha\nu$ pair. At 994° , the α peak is shifted slightly toward the $(\bar{2}20) \alpha\nu$ reflection and may have lost some intensity. At 960° , the (220) α is little more than a low angle shoulder on the $\alpha\nu (\bar{2}20)$. At 930° the conversion to $\alpha\nu$ appears complete. We are observing here the conversion $(\sigma + \alpha) \rightarrow (\alpha\nu + \alpha)$. It appears that when $\alpha\nu$ grows to about 75% of the whole, the remaining alpha converts to $\alpha\nu$ only after oxidation to some composition greater than $\alpha\nu$ has occurred. It seems quite clear in this experiment and those following that the conversion of α to $\alpha\nu$ is essentially complete well above 900° (on the oxidation cycle) and one is very hard pressed to explain the X-ray data in terms of the tensimetric results. As shown in Figure 1, the thermograms show a higher composition on the oxidation cycle until about 825° . It is necessary that as much as 40% α be present to give the compositions indicated by the tensimetric work at temperatures where only $\alpha\nu$ is seen by X-rays. This problem has not been resolved.

Heating at 500 mm O₂ Pressure, Run 38.--At the conclusion of Run 37 the sample was taken through another heating-cooling cycle in an effort to determine the seriousness of the contamination problem since there was evidence that this sample had undergone some reaction with the substrate. Although the fresh sample (Run 36) decomposed to σ at 1123° and 730 mm O₂, the reacted sample was not completely reduced to σ even at a pressure of 150 mm O₂ and a temperature of 1140°. In the course of the run, several competitive reactions appeared to be taking place, one of which was probably $\alpha z \rightarrow \alpha$.

Cooling at 730 mm O₂ Pressure, Run 39.--At the end of the 500 mm heating branch of the cycle the sample was pumped on (at 1200°) until the C \rightarrow A transformation occurred (not completed). The pressure was then adjusted to 730 mm O₂ and the 220 reflection was observed while cooling. The scans are shown in Figure 3. At 1091° a low angle shoulder appears which grows with continued cooling at the expense of the main peak. At 1050° the main peak is clearly split. We are observing then the growth of αz in a phase having a smaller lattice parameter and therefore higher composition. The only phase of higher composition known at this temperature is α . The $\sigma \rightarrow \alpha$ conversion thus must have occurred as the pressure was increased from the vacuum condition to 730 mm O₂. According to the thermogravimetric data, the $\sigma \rightarrow \alpha$ oxidation does not occur until under 1100°. At 1021°, the diphasic condition is still evident but by 989° the α phase is seen only as a low angle shoulder on the αz ($\bar{2}20$). Although not as clearly seen as in the 500 mm run there does appear to be some shift of the α peak to higher 2θ values relative to the αz peak positions indicating oxidation. The last scan at 941° shows only slight evidence of α . The asymmetric form of the double peak should be noticed.

Heating at 735 mm O₂ Pressure, Run 41.--The (220) reflections as a function of temperature is shown in Figure 4. The pure α peak is shown at 779°. At 881° conversion to α_z is about 50% complete. At 924° α is still in the oxidized form and is not clearly separated from the α_z ($\bar{2}20$), but at 1005° the shift to lower 2θ is pronounced, with the α peak near the center of the α_z ($\bar{2}20$) - (220) doublet. The shift to lower 2θ continues as the temperature is increased with no significant intensity changes. At 1090° the α (220) and α_z (220) peaks almost overlap. At 1105°, the reduction to σ is observed as a decrease in the α_z ($\bar{2}20$) intensity and by 1133° there appears to be only one phase present (σ), though poorly crystallized.

Cooling at 635 mm O₂ Pressure, Run 41.--On the cooling cycle there appears to be a very broad low angle shoulder at all temperatures which is presently attributed to a reaction with the alumina support. At 1135° the main peak appeared to be single, but at 1087° it was split equally with a peak separation of 0.10° 2θ . Although presence of the α_z (220) reflection is not clear, peak positions indicate that the low angle peak must be α , the high angle peak being the α_z ($\bar{2}20$). Here again the $\sigma \rightarrow \alpha$ conversion occurred as the pressure was raised. At 1081° the growth of α_z is more clearly seen by the appearance of a low angle shoulder. The growth is rapid and at 1067° only about 20% α remained. As the temperature was further lowered, the α peak shift was not clearly seen, but in comparing the 1038° and 1011° scans there again is some indication of a shift to higher 2θ values, demonstrating the $\alpha_{\text{red}} \rightarrow \alpha_{\text{ox}}$ reaction. At 920° there appeared to be only the α_z pseudophase.

Heating at 20 mm O₂ Pressure, Run 42.--A 20 mm oxidation-reduction cycle was made for purposes of comparison. As shown in Figure 5, with heating, the reduced phase appears initially on the low angle side of the main peak. The observed break to σ at 936° is nearly the same as found in the tensimetric work (932°).

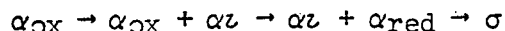
Cooling at 20 mm O₂ Pressure, Run 42.--The usual low pressure transformation with cooling from the σ region is seen as a growth on the high angle side of the main peak. It should be noted that the $\sigma \rightarrow \alpha$ oxidation at 904° agrees well with the 910° temperature observed in the tensimetric work.

Heating and Cooling Cycles at 732 mm O₂ Pressure on a Platinum Base, Run 45.--Since there appeared to be a contamination problem at the temperatures reached in these experiments, a run was made on a platinum base. The results as shown in Figures 7 and 8 give the same information as seen using the alumina base. The sample did not adhere well to the Pt and the run was hampered by the appearance of the Pt (200) line (not shown in the figures) on the low angle side of the (220) oxide reflections.

Discussion.--The tentative interpretation of the results thus far obtained is not in complete agreement with those made in the tensimetric work. The agreement between runs on Pt and alumina bases is good in that identical phase changes are observed, however, there does appear to be a temperature shift of as much as 50° which is not explained.

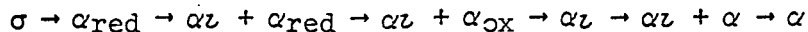
In general, on a heating run, the growth of $\alpha\alpha$ in α is slow. As the temperature is raised, as shown in Figure 9, the position of the α (220) peak and hence its lattice parameter changes regularly. It is

not clear at this time whether or not there is a change in slope of the parameter vs temperature curve as is suggested by the data when α becomes a minor second phase. If it is assumed that when an alpha peak is situated at the center of the αz doublet their compositions are the same, it is necessary that at the higher temperatures, alpha has a lower composition than αz or that an $\alpha \rightarrow \sigma$ transition occurs without any apparant discontinuity. It does not seem that the a priori assumption is necessarily correct but that at equal compositions the α parameter may be larger than that of αz . Thus as the α (220) peak moves almost under the αz (220) reflection, it is not necessary that the overall composition fall below that of what we will call a "pure" αz pseudophase. At this point there is no clear evidence for a complete conversion to alpha as suggested by the tensimetric work. In summary then, the observed changes with reduction are:



With cooling, a complete $\sigma \rightarrow \alpha$ change is seen only indirectly by the growth of αz on the low angle side of the (220) reflection. The anomalously high position for the (220) reflection at this stage may be related to a difference in lattice parameter between pure α and that of α when a minor phase. As indicated by the dotted line in Figure 9, the lattice parameter in the former case may be smaller than for the latter. As the temperature is lowered there is only a slight shift of the α peak to higher 2θ (relative to the αz doublet) before what appears to be nearly complete conversion to αz occurs. On the basis of the X-ray data one would have to conclude that at 920° for example, there is more alpha on the reduction path than in oxidation which is contrary to expectations from the TGA work.

The positions of the two αz peaks do not appear to be much shifted in comparing heating and cooling scans at similar temperatures. The changes seen with oxidation are:



Although there is no direct observation of either $\sigma \rightarrow \alpha$ or $\alpha z \rightarrow \alpha$ to the extent seen in the tensimetric work, there is little doubt that both reactions do occur.

There are some points which are worthy of further discussion. In the preceding account no mention of the pure z phase has been made. There is no X-ray evidence (and also no tensimetric evidence) that one ever obtains a pure z phase at these higher pressures. The question as to what really is this pseudophase (αz) cannot be answered here but there are perhaps a few pertinent points. It is observed that the ($\bar{2}20$) peak of the rhombohedral doublet is of greater intensity than the (220) for the αz phase, whereas for pure z these reflections must have equal intensity. The simplest explanation for this which also explains nicely the higher composition observed is that an α (220) peak is hidden under the z ($\bar{2}20$) envelope. There is little change in the intensity ratio of this doublet with change in temperature which would mean that the "hidden" alpha phase is extraordinarily stabilized with respect to reduction. There is evidence already discussed that another kind of α is also somehow stabilized (since it does not convert to αz) but that this α is subject to oxidation and reduction. The extraordinary stabilization requirement makes the simple answer not very acceptable. It is hoped that the high resolution Nonius-Guinier camera will give a more clear understanding of this region.

Lattice Expansion of α as a Function of Pressure

Lattice parameters of the disordered α phase have been determined at 638° as a function of oxygen pressure (Run 44). As shown in Figure 10, there is a regular variation. The correlation of parameter to composition will be made as the data becomes available from the detailed tensimetric study presently being made.

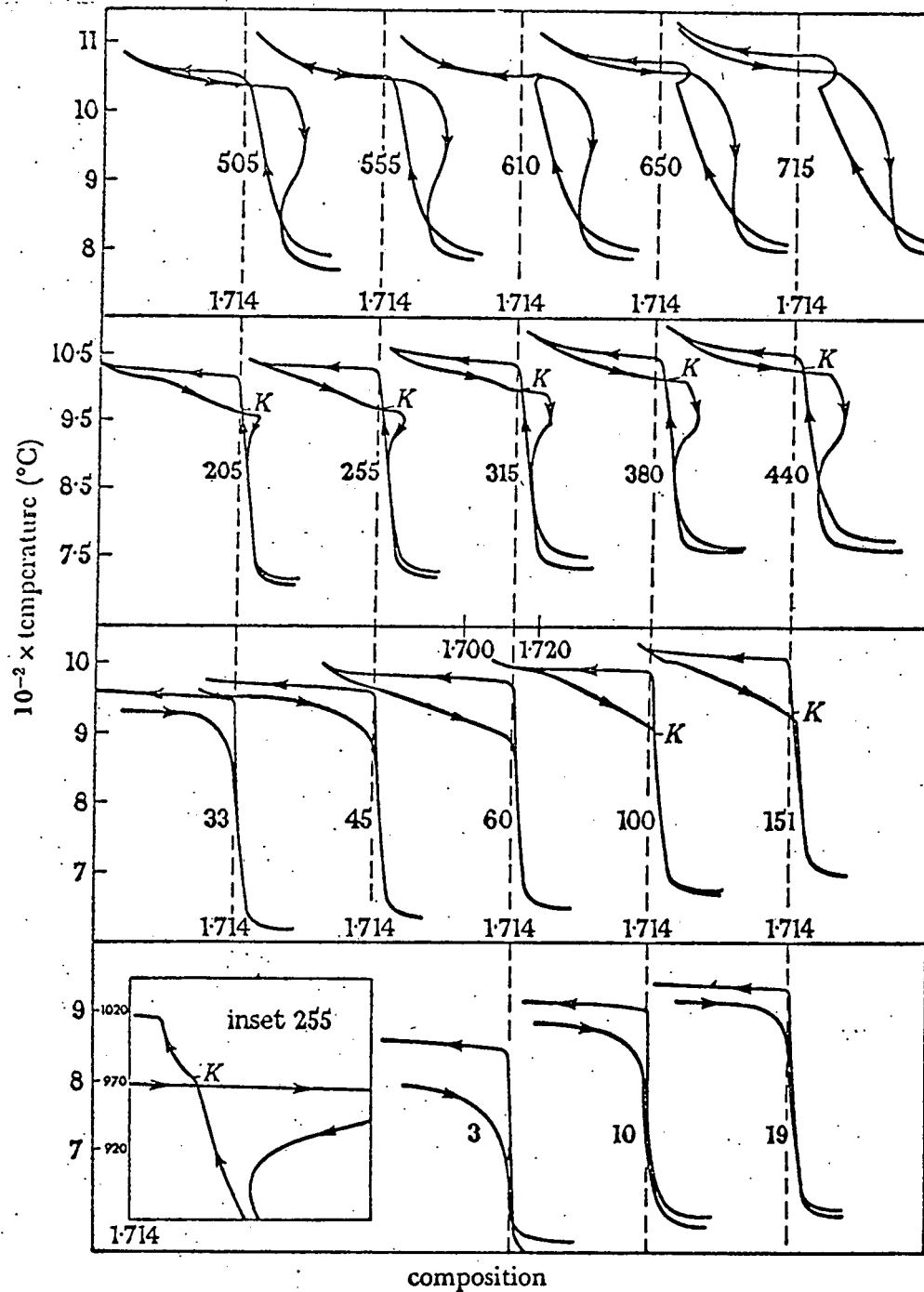
The Nonius Guinier-Lenne High Temperature Camera

A new Nonius Guinier-Lenne high temperature camera has been aligned and a number of preliminary exposures taken. Resolution is sufficient to distinguish the fine splitting of the main lines of all the ordered phases. Superstructure reflections are also seen with longer exposures and the temperatures of phase changes as observed with the new camera at a heating rate of less than $2^\circ/\text{hr}$ agree well with those determined by the tensimetric method.

The vacuum system shown in Figure 11 enables control of pressures in the ranges 1×10^{-9} - 5×10^{-3} mm (via the ion gauge and Granville Phillips leak valve) and 1 - 800 mm (with the Wallace and Tiernan dial manometer). The system has been pumped down to 3×10^{-5} torr and the pressure on a 10 mm run did not appear to change over a period of four days.

REFERENCES

1. Hyde, B. G., Bevan, D. J. M., and Eyring, L., Phil. Trans. Roy. Soc., A 259, 583 (1966).
2. Burnham, D. A., Thesis, Arizona State University (1967).



Portion of isobars in the composition range *ca.* $\text{PrO}_{1.68}$ to $\text{PrO}_{1.74}$ on an expanded composition scale. (The run number against each curve is the nominal oxygen pressure in torr.)

Figure 1

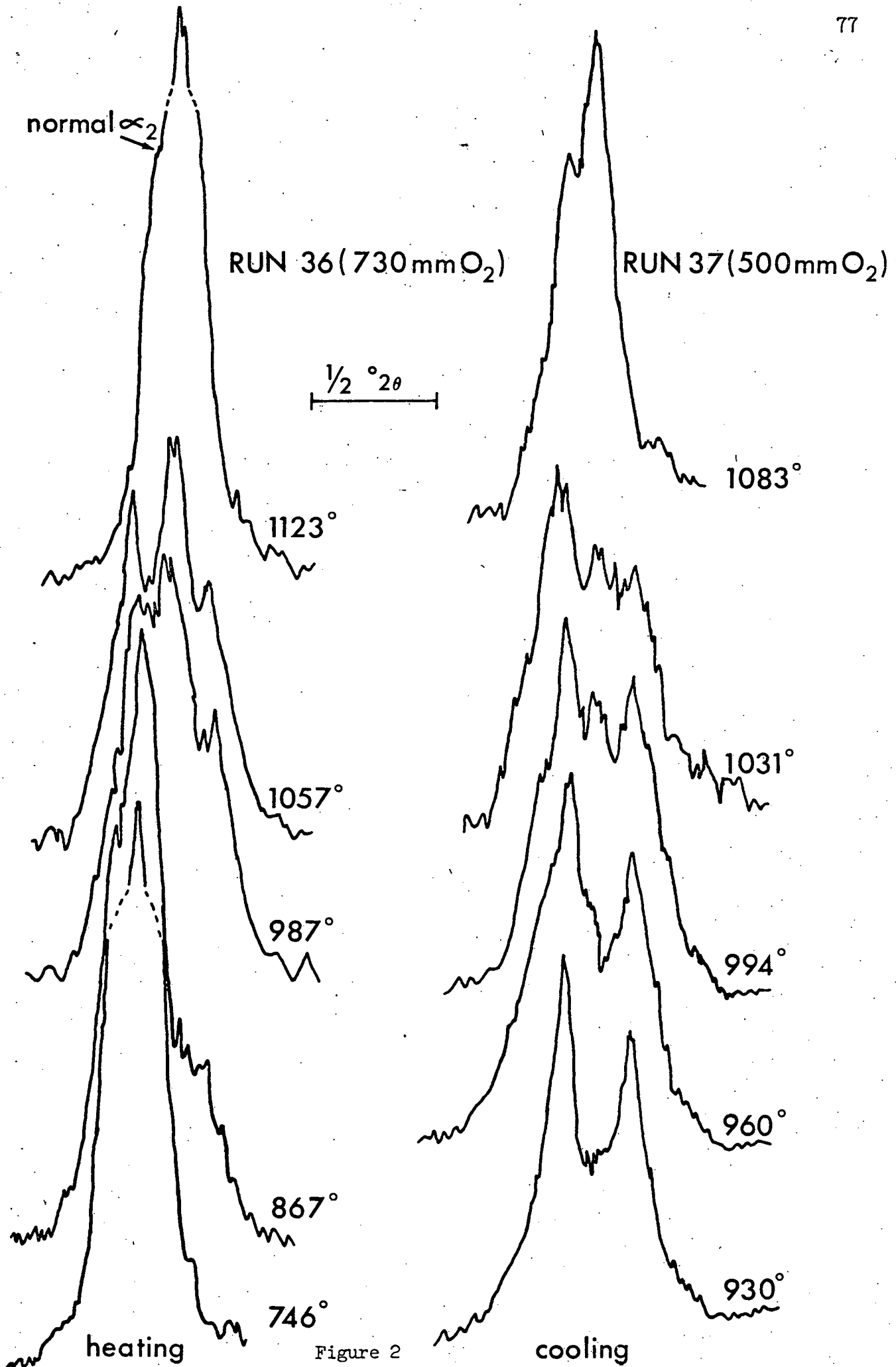


Figure 2

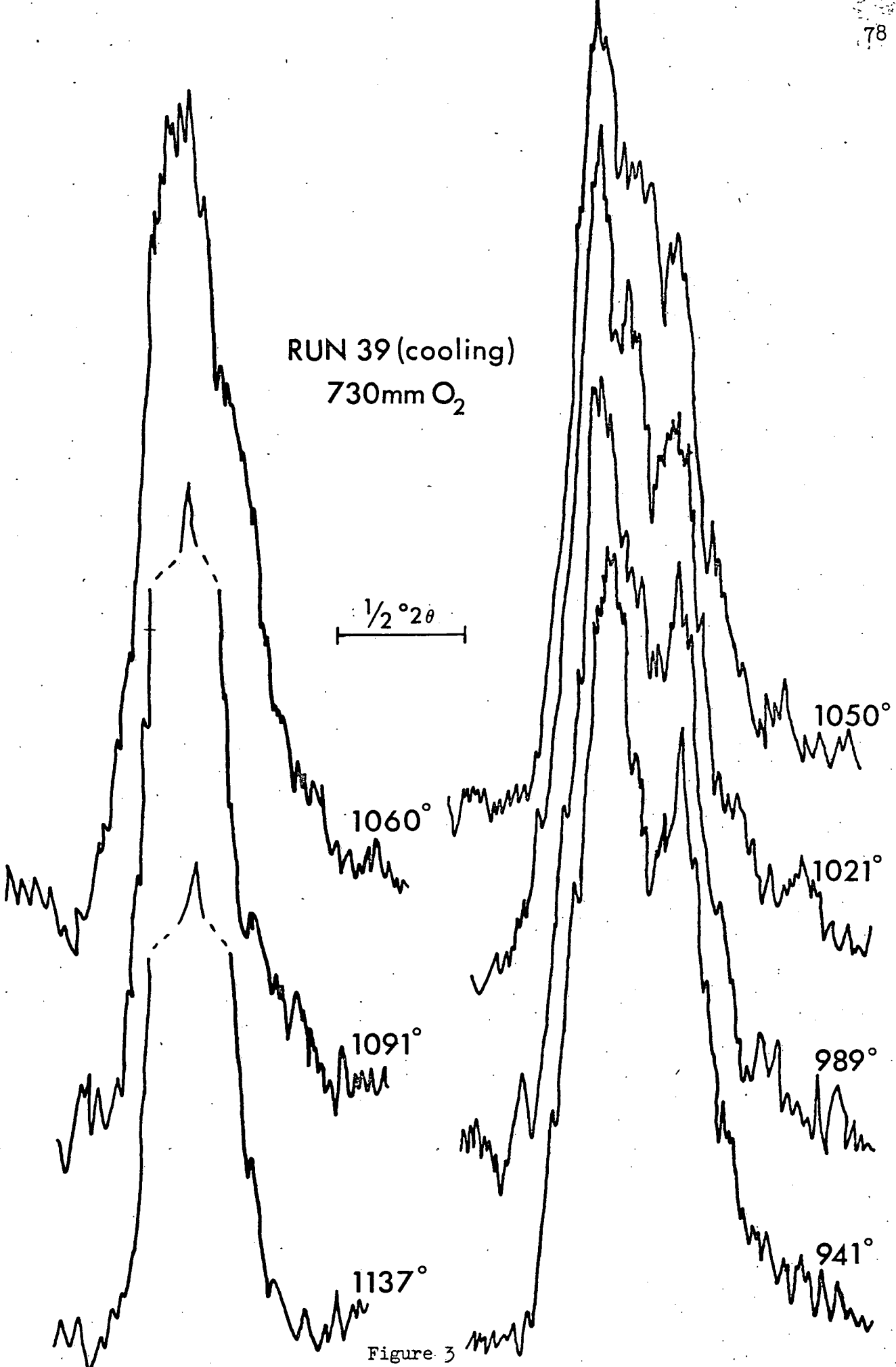


Figure 3

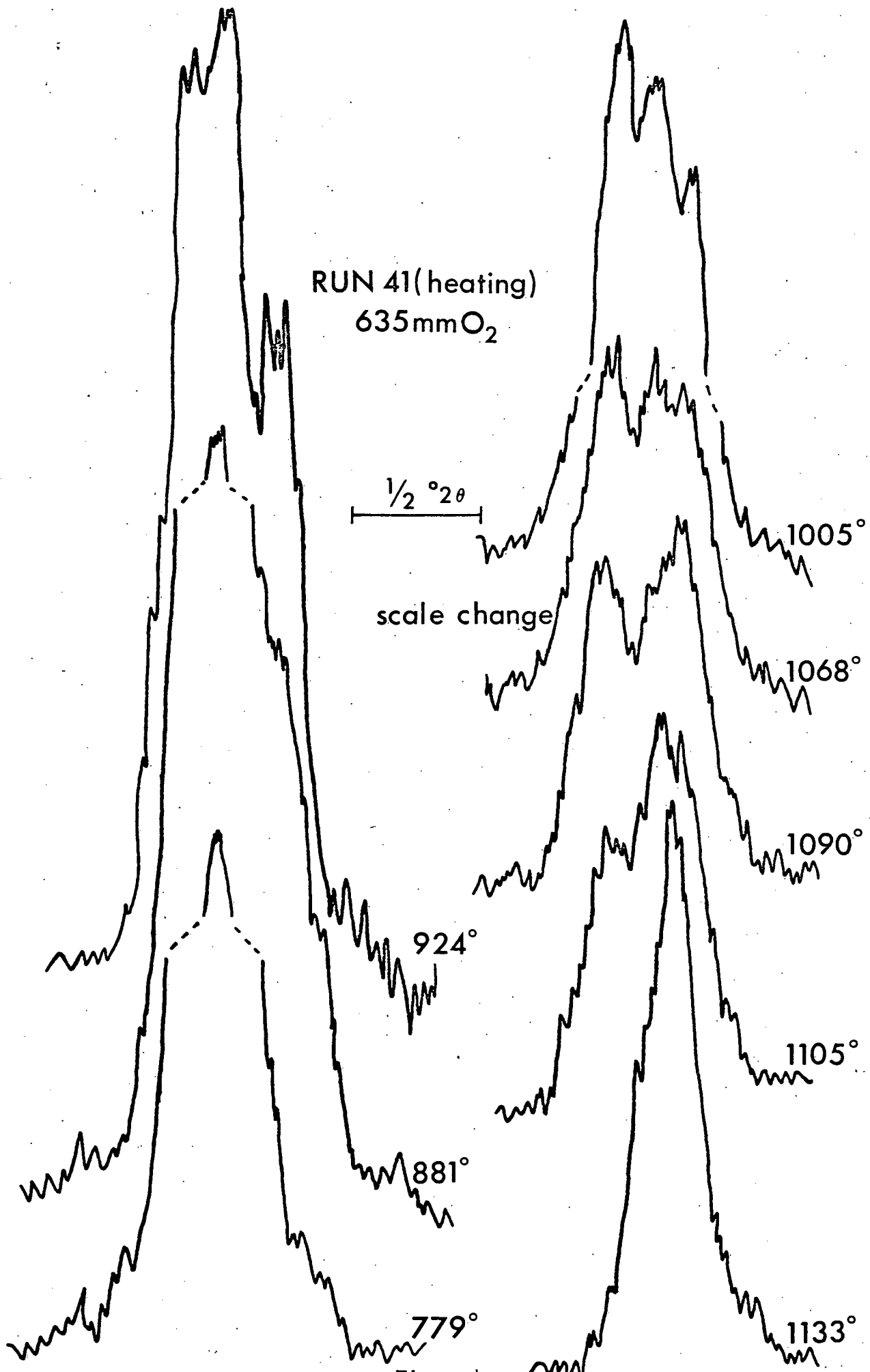


Figure 4

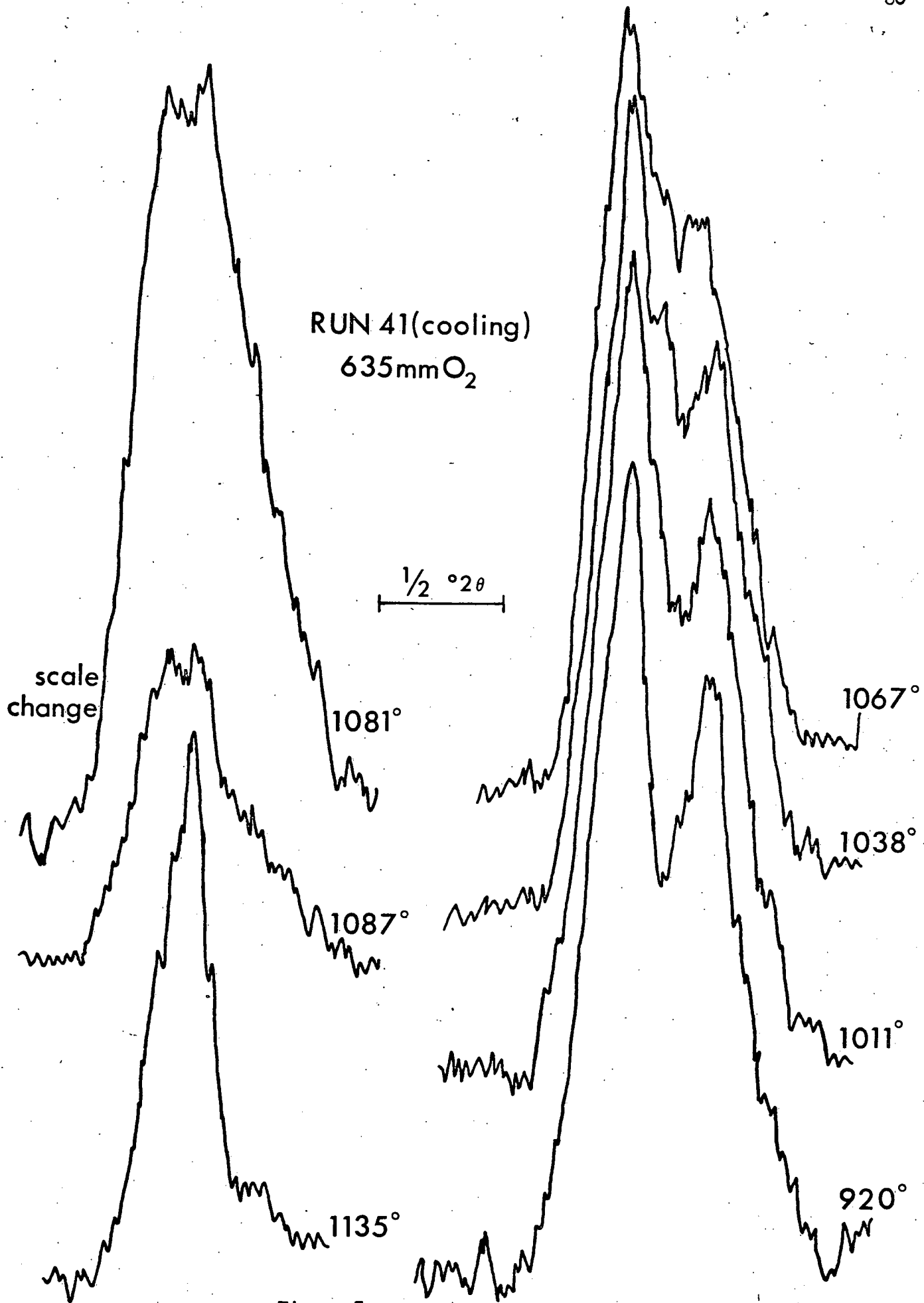


Figure 5

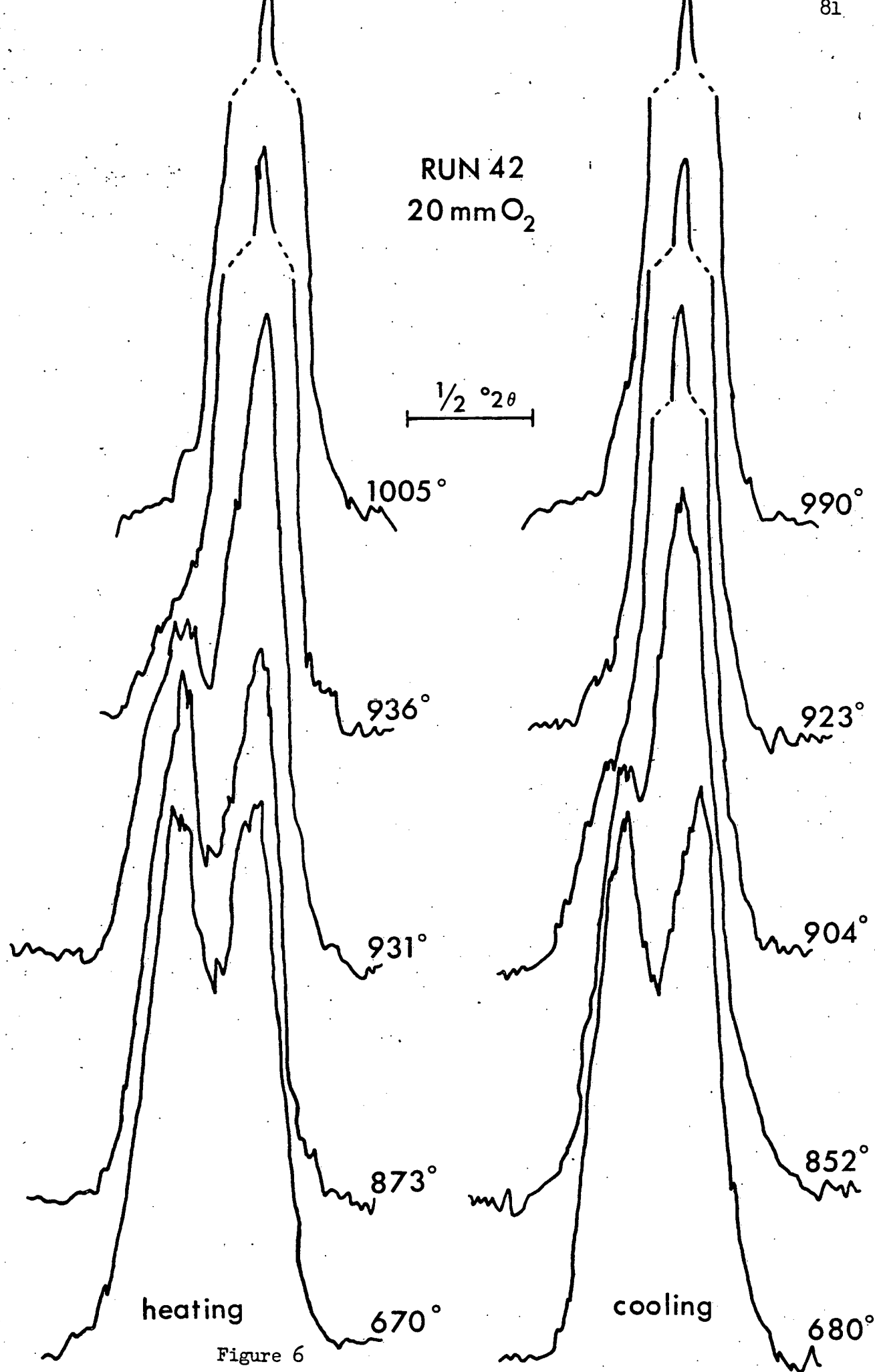


Figure 6

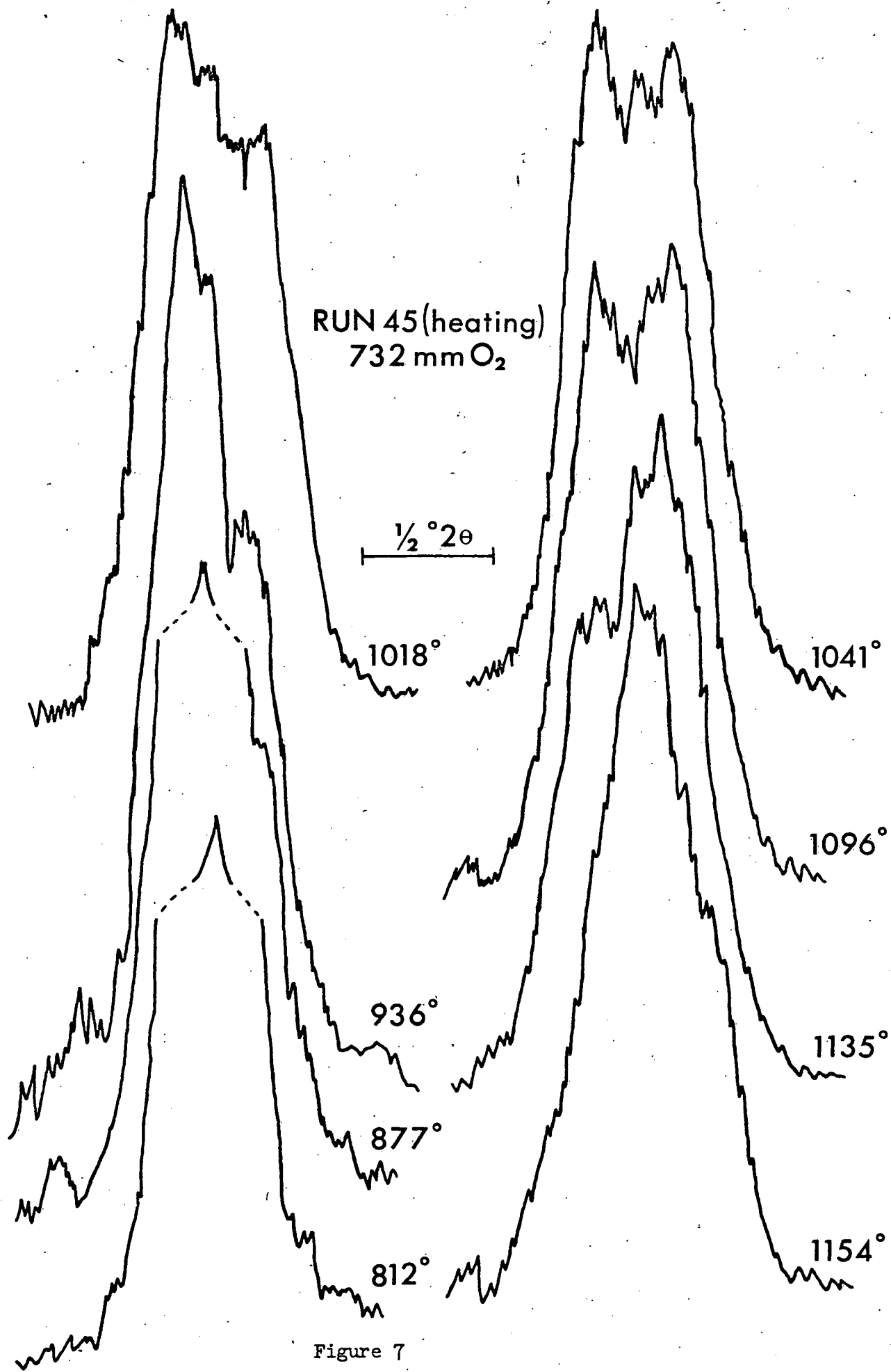


Figure 7

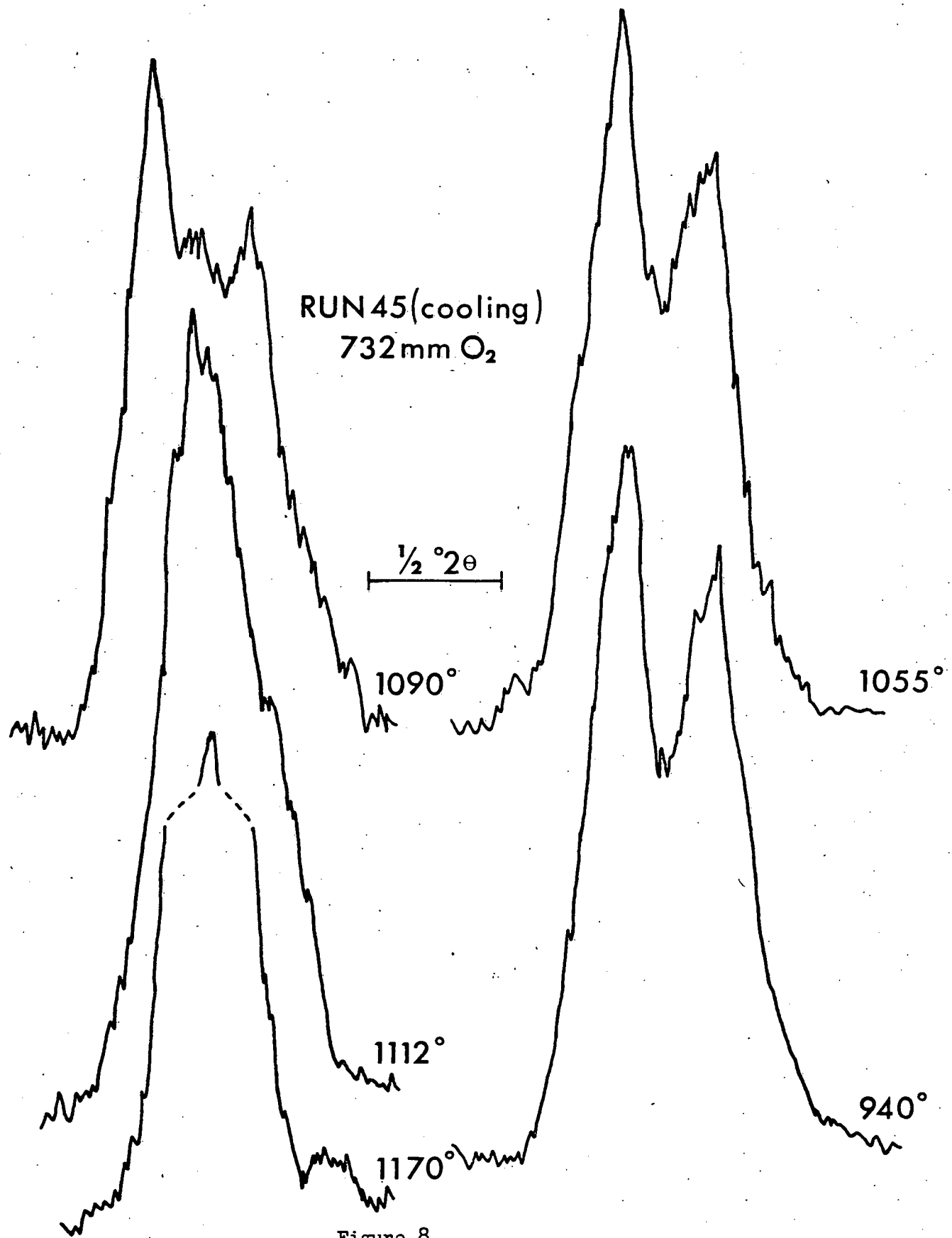
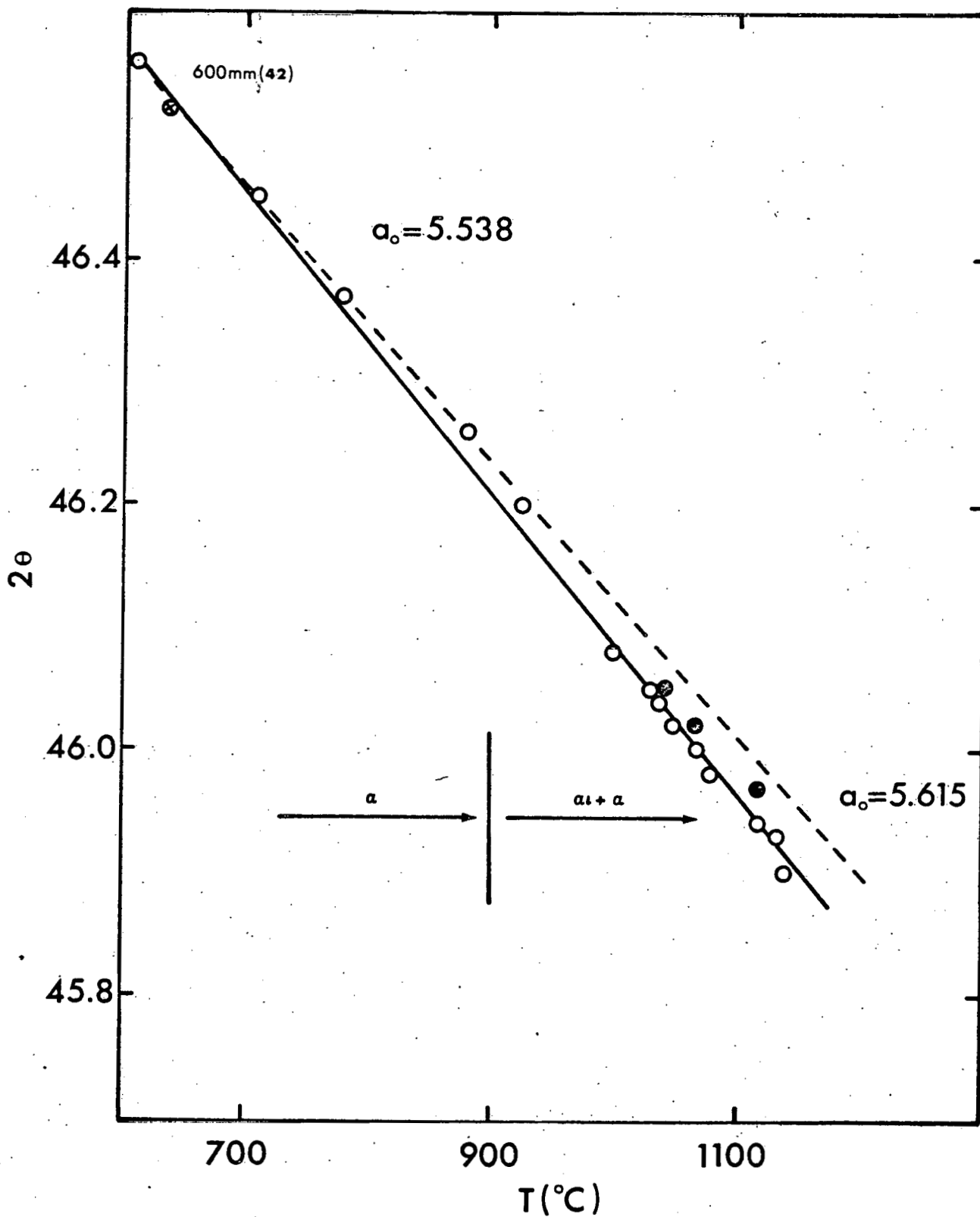


Figure 8

Alpha 220 Line Position



RUN 41, 635 mm O₂ (○ heating, ● cooling)

Figure 9

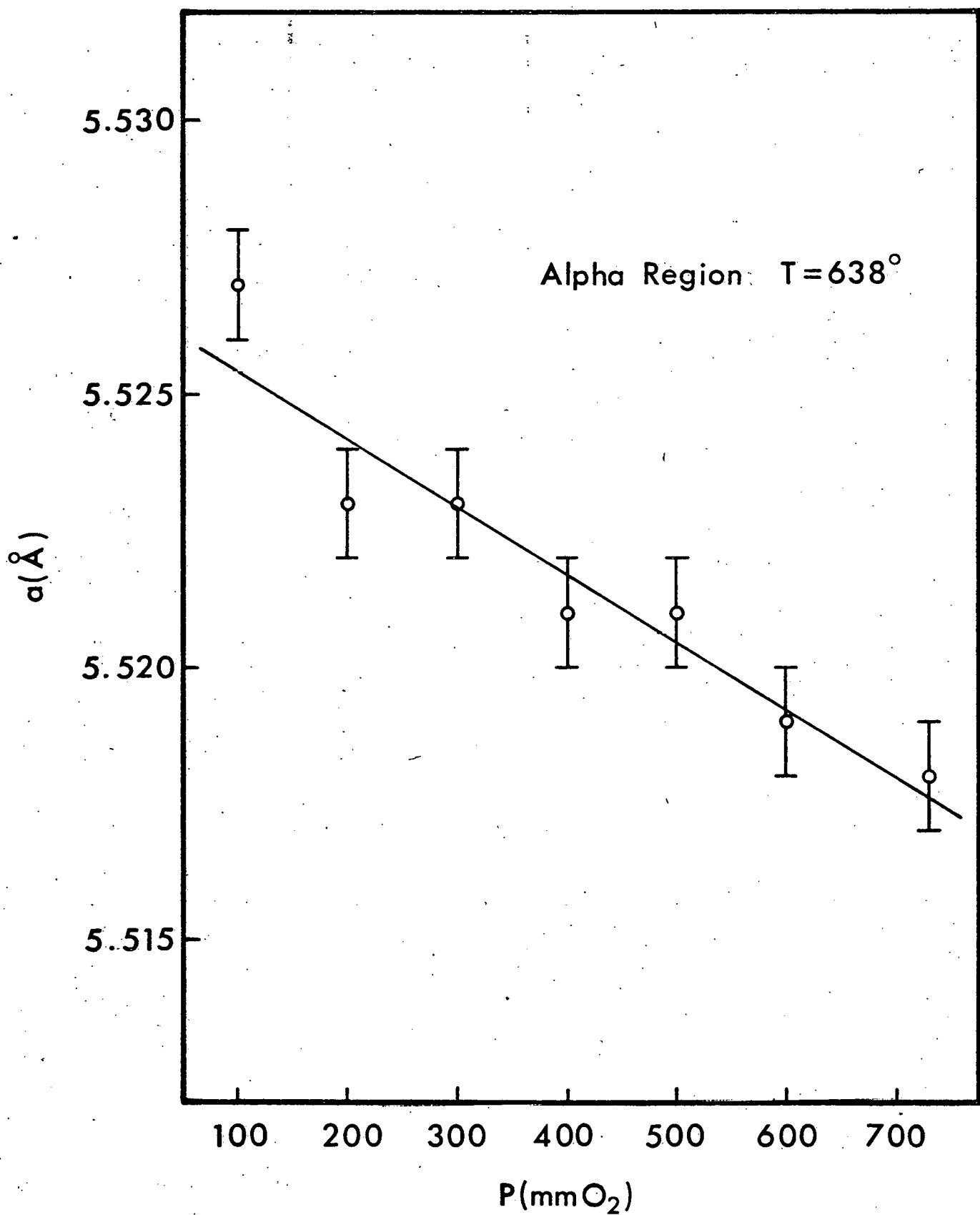


Figure 10

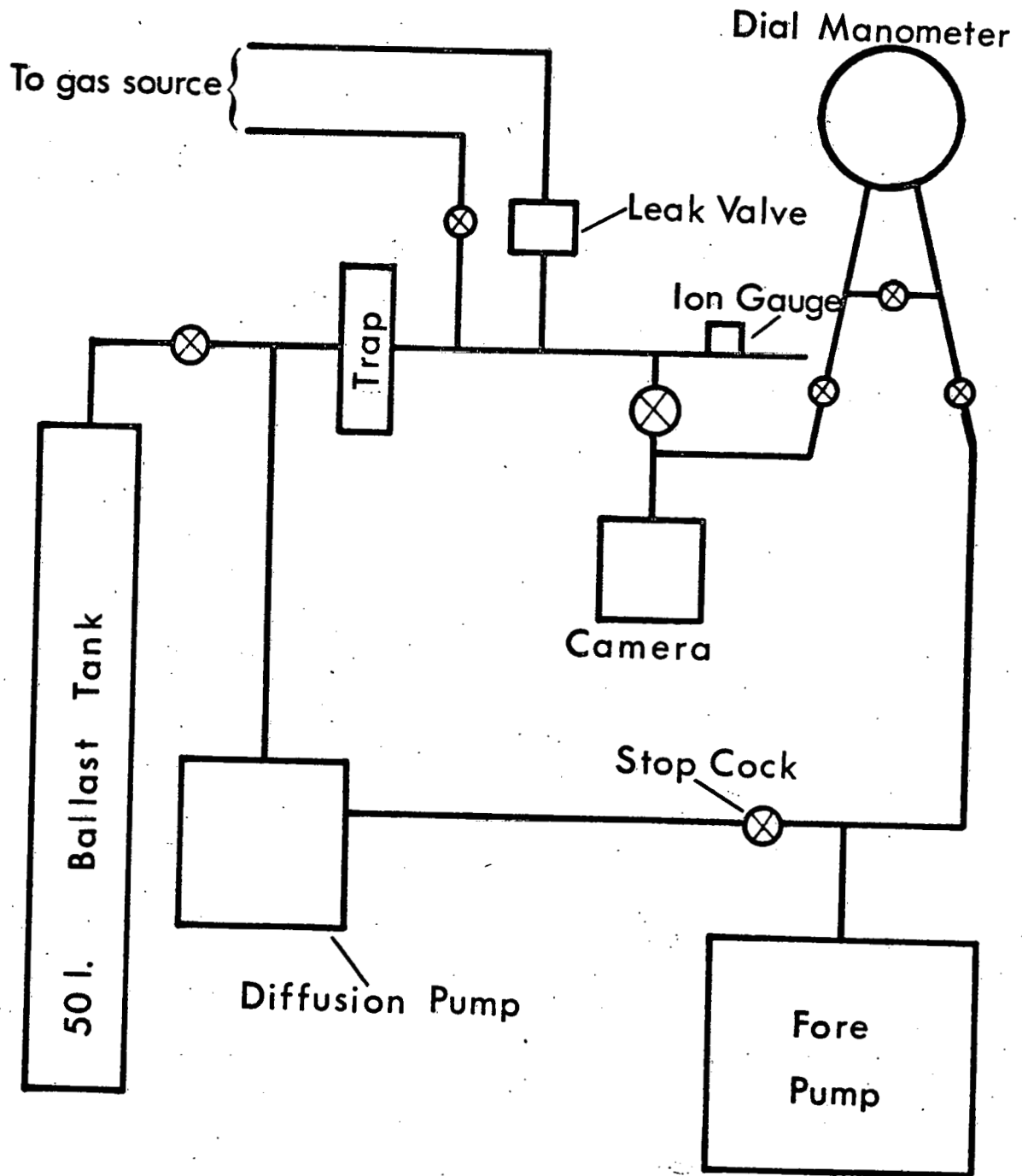


Figure 11

EXPERIMENTAL PROGRAM FOR CRYSTAL GROWING
OF RARE EARTH OXIDES

As described in the last technical progress report¹ experiments were started to grow single crystals of various praseodymium oxides. Further experiments in this direction were carried out, using the plasma-torch, various salt-melts and the hydrothermal method.

The experiments with the plasma-torch showed that with argon/oxygen it was not possible to get a single crystal of praseodymium oxide, whereas it was possible to get small single crystals of A-form Nd_2O_3 . With argon/hydrogen it may be possible to obtain Pr_2O_3 in the A-form.

The experiments with different salt-melts under atmospheric conditions gave evidence that only single crystals of the A-form praseodymium oxide or compounds of praseodymium with components of the flux would be synthesized. A series using techniques already developed^{2,3,4} for growing single crystals of CeO_2 and/or ThO_2 were carried out to check these methods for applicability in growing single crystal praseodymia. The results of these runs are shown in Table I. A heavy walled covered platinum crucible 3 cm by 10 cm was used as a container. Although the methods worked satisfactorily for cerium dioxide, praseodymium in the trivalent state reacted with components of the flux to form compounds. It is conceivable that if the crystallization could be realized at oxygen activities sufficiently high to assure the praseodymium in the tetravalent state, higher oxide crystals of praseodymium could be grown.

Other experiments with the lead fluoride-bismuth oxide and lithium oxide-tungsten oxide melts showed that the temperature in the first must

Table I. Rare Earth Oxide Crystal Growth from Salt Melts

Run No.	LnO _x	Mole per cent Bi ₂ O ₃	PbF ₂	High Temp	Low Temp	Soak Time	Cooling Rate	Comments
1	CeO ₂ 7.4	14.8	77.8	1250°	900°	15 hrs	5°/hr	Regular amber colored CeO ₂ cubes 2 mm on an edge, fluorite structure, a = 5.418.
2	CeO ₂ 7.4	14.8	77.8	1235°	890°	15 hrs	5°/hr	CeO ₂ crystals which were more irregular than the last. Tendency to be in clusters of small interlocking cubes. X-ray diagram the same as run # 1.
3	PrO _{1.83} 7.4	14.8	77.8	1250°	895°	15 hrs	5°/hr	Small, transparent, yellow particles; no regular shape, about .05 mm across, principle phase fluorite.
4	PrO _{1.83} 13.8	13.8	72.4	1250°	900°	10 hrs	5°/hr	Similar yellow particles rather spherical in shape, fluorite phase a = 5.417, weak unknown second phase.
5	PrO _{1.83} 24.2	12.1	63.6	1200°	910°	12 hrs	5°/hr	Yellow material, similar in size and color.
6	PrO _{1.83} 24.2	12.1	63.6	1115°	890°	4 hrs	5°/hr	Glassy, yellow fragments.

Table I. (Cont.)

Run No.	LnO _x	Mole per cent			High Temp	Low Temp	Soak Time	Cooling Rate	Comments
7	CeO ₂ 4.7	LiOH·H ₂ O 37.4	H ₃ BO ₃ 38.8	MoO ₃ 19.2	1270°	900°	10 hrs	5°/hr	White transparent crystals octagonal in form, fluorite a = 5.412.
8	PrO _{1.83} 14.6	33.5	34.7	17.2	1330°	1050°	15 hrs	3°/hr	Very green, transparent needles about 3 mm long, extremely complex X-ray pattern.
9	PrO _{1.83} 28.4	23.5	--	WO ₃ 48.2	1320°	1065°	15 hrs	3°/hr	More green, transparent material slightly crystalline in structure sharp X-ray diagram of great complexity.
10	PrO _{1.83} 20.8	PbF ₂ 26.4	26.4	PbO 26.4	1295°	1045°	17 hrs	3°/hr	Small, slightly green, transparent material irregularly shaped, complex X-ray diffraction pattern of same phase as in run # 8.
11	PrO _{1.83} 20.0	41.6	--	38.4	1275°	1050°	18.5 hrs	5°/hr	Small (1 mm) irregularly shaped, transparent yellow particles. Similar in form to those of run # 4. Strong lines are a fluorite pattern of smaller parameter than run # 4.

be higher than 900° to grow crystals and in the second higher than 1200° . It was found that in the second melt the rare earth oxide reacted with the $\text{Li}_2\text{O}\cdot y\text{LnO}_x\cdot z\text{WO}_3$ liquid below 1200° to form an incongruently melting compound of $\text{Li}_2\text{O}\cdot y\text{LnO}_x\cdot z\text{WO}_3$ with $x = 1.5$ for praseodymium and $x = 2$ for cerium. In both of the above melts it is only possible to grow the A- Pr_2O_3 .

A more suitable salt-melt was sought which would permit the work to be carried out at a lower temperature so as to obtain the C-form of the oxide. A literature survey⁵⁻⁷ showed that the system lead oxide-bismuth oxide might be suitable for growing C-form and also $\text{PrO}_{1.833}$. In an experiment with 68 Mol % PbO , 27 Mol % Bi_2O_3 and 5 Mol % $\text{PrO}_{1.83}$ at 850° and a cooling rate of 3° per hour for 25 hours, hexagonal shaped crystals of A- Pr_2O_3 of about 1 mm size were formed. But at 800° , using the same conditions, no crystals are formed, and the X-ray pattern gave evidence for the A- Pr_2O_3 . Therefore, it seems that Pr_2O_3 crystals are formed at atmospheric conditions only at higher temperatures than 800° and at this temperature it is only possible to prepare crystals of the A-form.

Failure of experiments with the plasma-torch and salt-melts to produce Pr_2O_3 crystals in the cubic habit leave the hydrothermal method as more likely to yield single crystals of C- Pr_2O_3 . Alternatively, salt-melts under oxygen pressure might be used. Very slow oxidation of a C- Pr_2O_3 crystal at low temperature might then yield crystals of PrO_x with $x > 1.5$.

The equipment for most of the high pressure experiments was made in this laboratory. O-ring sealed vessels of 17-4 PH stainless steel (chromium-nickel steel) with a tensile strength of 165,000 psi were used. The autoclaves having 1" I.D., 2" O.D., and a length between 4" and 12" were operable up to 20,000 psi with a safety factor of three. For an

experiment at temperatures higher than 700° the same type of autoclave was used with a small platinum-wound furnace inside, the outside being water cooled. The current and thermocouple leads were brought through 1/8" holes in the wall and sealed with epoxy-resin of good tensile strength. However, this type of seal is unsuitable at the higher temperatures since the epoxy reacts explosively with pressurized oxygen.

All experiments were carried out behind a thick steel wall. The voltage regulator for the furnace, the potentiometer for the thermocouple and the mechanism for opening the valve and the mechanism for quenching the autoclave were arranged in such a way behind the wall that all experiments could be carried out in safety. The pressure gauge could be read from behind the wall by means of mirrors.

Experiments with the System Pr₂O₃-H₂O.--The first two hydrothermal runs were performed in a way similar to the hydrothermal crystal growth of Al₂O₃ and SiO₂^{8,9} in equipment supplied by Autoclave Engineers, good for 50,000 psi, but limited to temperatures below 500°. The starting material in the first run was PrO_{1.83} and 3N Na₂CO₃. The contents of the vessel were heated at 395° for 60 hours with 22,000 psi, this pressure being achieved by using a special pump.¹⁰ The second run was carried out with PrO_{1.83} and 1N NaOH at 450° for 60 hours with 40,000 psi.

In both runs the product was found to be an oxyhydroxide and not an oxide as was the case for the system SiO₂-H₂O and Al₂O₃-H₂O under identical conditions. The X-ray pattern indicated in Table II of this praseodymium oxyhydroxide was very similar to the pattern of NdOOH, formed under similar conditions, synthesized by Shafer and Roy.¹¹

Table II. X-ray Pattern of PrOOH (form I)

2θ	d	I
21.0	4.23	20
21.6	4.11	25
27.35	3.26	30
29.6	3.02	50
30.9	2.89	100
32.0	2.80	20
38.1	2.36	5
42.85	2.11	5
45.6	1.99	25
48.4	1.88	30
51.0	1.79	20

This experiment showed that it would be advantageous to first establish the phase diagram for the system $\text{Pr}_2\text{O}_3\text{-H}_2\text{O}$ before proceeding with more hydrothermal experiments for growing crystals.

In most of the runs $\text{Pr}(\text{OH})_3$ was used and was prepared under argon to avoid the formation of the carbonate. The hydroxide was placed in a platinum crucible and lightly closed. After putting the crucible in the autoclave, the vessel was filled with water to about 70-85% of its volume, closed and then heated. To avoid rehydration after the run, the samples were both pressure and temperature quenched by opening the valve of the hot bomb to the atmosphere and allowing the water to escape quickly as vapor. The vessel was then cooled rapidly by immersing it in cold water. The success of this method depends on the fact that the hydrates do not decompose rapidly at temperatures near their equilibrium dehydration temperature in the absence of water. The products were examined by powder X-ray diffraction and spectral observation between 25,000 Å and 3500 Å. Table III summarizes the runs made.

Table III. Data for the System $\text{Pr}_2\text{O}_3\text{-H}_2\text{O}$

<u>Temp[°C]</u>	<u>Pressure[psi]</u>	<u>Time[hr]</u>	<u>Initial condition</u>	<u>After run</u>
300	8000	18	$\text{Pr}(\text{OH})_3\text{-gel}$	$\text{Pr}(\text{OH})_3$
350	5000	25	A- Pr_2O_3	$\text{Pr}(\text{OH})_3$
395	22000	60	$\text{PrO}_{1.833}$	PrOOH (form 1)
450	40000	60	$\text{PrO}_{1.833}$	PrOOH
500	4000	25	$\text{Pr}(\text{OH})_3$	PrOOH
650	6000	15	A- Pr_2O_3	PrOOH
680	7000	140	$\text{Pr}(\text{OH})_3$	Oxyhydroxide (form 2)
750	8000	10	$\text{Pr}(\text{OH})_3\text{-gel}$	blow up

The above data would suggest the following phase diagram:

The results of these few experiments in the system $\text{Pr}_2\text{O}_3\text{-H}_2\text{O}$ gave evidence that only at temperatures higher than 700° will it be possible to use the hydrothermal method for growing single crystals of C-type Pr_2O_3 . Below this temperature the oxides $\text{Pr}_2\text{O}_3\cdot\text{H}_2\text{O}$ and $\text{Pr}_2\text{O}_3\cdot 3\text{H}_2\text{O}$ are formed. The suggested range for synthesizing C- Pr_2O_3 is about $750^\circ\text{-}800^\circ$ and 5000 to 10,000 psi. The present equipment is inadequate and new equipment is necessary at these higher temperatures, since the tensile strength of the externally heated vessel is not high enough as can be seen from the last experiment of Table III.

In an experiment with $\text{Nd}(\text{OH})_3\text{-H}_2\text{O}$ at 680° and 7000 psi single crystals, very thin needles of about 2 mm, were formed within 85 hours. But in an experiment with $\text{Pr}(\text{OH})_3\text{-H}_2\text{O}$ under the same conditions only oxyhydroxide was formed. The X-ray pattern was different from the pattern of PrOOH , synthesized at lower temperatures. It seems that shortly before the transition from PrOOH to the C- Pr_2O_3 a high temperature form of $\text{Pr}_2\text{O}_3\cdot\text{H}_2\text{O}$ or a less hydrated oxide, as for example $\text{Pr}_2\text{O}_3\cdot 1/2\text{H}_2\text{O}$, is formed. The X-ray pattern is recorded in Table IV.

Table IV. X-ray Pattern of Praseodymium Oxyhydrate (form II)

<u>2 θ</u>	<u>d</u>	<u>I</u>
15.85	5.59	10
17.8	4.98	0.5
27.0	3.30	1.5
27.55	3.24	6
28.45	3.14	1.5
31.2	2.86	0.5
32.45	2.76	2
39.3	2.29	0.5
40.05	2.25	2
42.7	2.12	1
48.8	1.86	2.5
49.3	1.85	2

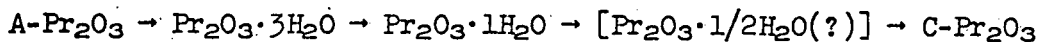
The phase diagrams of $\text{Nd}_2\text{O}_3\text{-H}_2\text{O}$ and $\text{Sm}_2\text{O}_3\text{-H}_2\text{O}$ deduced by Shafer and Roy⁹ found the transition of SmOOH to $\text{C-Sm}_2\text{O}_3$ to occur at about 600° and NdOOH to $\text{C-Nd}_2\text{O}_3$ at about 650° at a pressure of 7000 psi. The transition from the hydrated to the unhydrated Pr_2O_3 by comparison, assuming a uniform gradation in properties, should occur at about 700° .

Investigation of the Reversibility of R_2O_3 Transformations.--Shafer and Roy¹¹ found during their hydrothermal experiments that $\text{B-Sm}_2\text{O}_3$ transforms to $\text{C-Sm}_2\text{O}_3$ at 750° , 3000 psi in a 18 hour run, $\text{A-Nd}_2\text{O}_3$ transforms to $\text{B-Nd}_2\text{O}_3$ at 1008° , 4000 psi in 42 hours and $\text{B-Nd}_2\text{O}_3$ transforms to $\text{C-Nd}_2\text{O}_3$ at 850° , 5000 psi in 18 hours.

A few experiments were carried out with Nd_2O_3 and Pr_2O_3 to investigate this transition and to investigate the possibility of obtaining the $\text{C-Pr}_2\text{O}_3$ from $\text{A-Pr}_2\text{O}_3$.

<u>Starting material</u>	<u>After run</u>	<u>Temp[$^\circ\text{C}$]</u>	<u>Pressure[psi]</u>	<u>Time[hr]</u>
$\text{A-Pr}_2\text{O}_3$	PrOOH	650°	6000	15
$\text{A-Pr}_2\text{O}_3$	mainly $\text{Pr}(\text{OH})_3$	650°	6000	4
PrOOH	$\text{Pr}(\text{OH})_3$	300°	5000	20
$\text{A-Nd}_2\text{O}_3$	mainly NdOOH	650°	7000	7

These experiments showed that $\text{A-Pr}_2\text{O}_3$ did not convert directly to $\text{C-Pr}_2\text{O}_3$ under the conditions of these experiments. The following mechanism is proposed for obtaining $\text{C-Pr}_2\text{O}_3$ from $\text{A-Pr}_2\text{O}_3$:



The limiting factor in this sequence of events is that the temperature of the final step must be about 750° . This was not possible with the present equipment.

Attempts to Prepare a Higher Oxidation State of Praseodymium.--In 1925 the first report of a praseodymium(V) compound was published by Prandtl et al.,¹² but this work has not been repeated and up to this time

no compound with praseodymium in the (V) state is confirmed. Some experiments in this direction were carried out using oxygen, even though experiments with fluorine, carried out by a group in Los Alamos¹³ were not successful.

Fluorite-type PrO_2 might take up oxygen interstitially in a way similar to $\text{UO}_{2+\delta}$. If such a compound could be formed, it would probably be stable only at low temperatures. An oxidizing salt-melt of $\text{LiClO}_4\text{-AgClO}_3$ was chosen for this experiment at a temperature of 270° , since decomposition temperature of AgClO_3 is 270° . At this temperature atomic oxygen is formed which is in close contact with PrO_2 in the melt. With $\text{LiClO}_4\text{-KMnO}_4$ the experiment could be carried out at 240° , which is the decomposition temperature for KMnO_4 . The experiments were carried out in an autoclave with 10,000 psi oxygen pressure.

After temperature quenching, the autoclave was opened and a spectrum of the melt taken. But even with reflecting spectroscopy no lines were found in the UV-region, as would be expected (similar to La_2O_3) for compounds having no f-electrons.

It was also thought possible to produce a higher oxide of praseodymium in the following manner:

1. to produce the peroxide PrO_2 , where the praseodymium is in the three-state
2. to oxidize this peroxide at low temperature to $\text{PrO}_{2.5}$ with praseodymium in the four-state as is possible with $\text{PrO}_{1.5}$
3. to change the bonding by pressure and get Pr_2O_5 in this way with praseodymium in the (V) state.

The preparation of the praseodymium peroxide has been reported by Makarov and Soboleva.¹⁴ They precipitated $\text{PrOOH}(\text{OH})_2$ from $\text{Pr}(\text{NO}_3)_3\text{-H}_2\text{O}_2$ -solution with NH_3 and dehydrated the peroxyhydroxide with P_2O_5 under vacuum.

Bisi and Clerici¹⁵ precipitated $\text{Pr}(\text{ClO}_2)_3$ from $\text{Pr}(\text{NO}_3)_3$ -solution with NaClO_2 in alcohol and decomposed the praseodymium chlorite to the stable praseodymium peroxide.

The peroxide used in this experiment was prepared as described by Makarov and Soboleva. The first oxydation experiment at 80° and 7000 psi oxygen pressure for 2 days showed no reaction. Even at 120° and 10,000 psi oxygen pressure for several days no oxidation was observed. At 160° and 10,000 psi oxygen the peroxide PrO_2 was decomposed and the normal oxide PrO_2 was formed. No further attempts to produce praseodymium(V) oxides were tried.

References

1. Technical Progress Report AT(11-1)-1109, COO-1109-25, June 1967.
2. Vinokurov, I. V., Zonn, Z. N., and Ioffe, V. A., Soviet Physics-Solid State, 7, No. 4, October 1965.
3. Finch, C. B., and Clark, G. W., J. Appl. Phys., 37, 3910 (1966).
4. Linares, Robert C., J. Phys. Chem. Solids, 28, 1285-1291 (1967).
5. Levin, E. M., McMordie, H. F., and Hall, F. P., Phase Diagrams for Ceramists, The American Ceramic Society, Inc., 1956.
6. Laudise, R. A., Molten Salt Solvents in the Art and Science of Growing Crystals (ed. J. J. Gillman), John Wiley, New York, 1963.
7. Nassau, K., Crystal Growth Techniques, Bell Telephone, Inc., Murray Hill, New Jersey.
8. Ballman, A. A., and Laudise, R. A., Hydrothermal Growth in the Art and Science of Growing Crystals (ed. J. J. Gillman), John Wiley, New York, 1963.
9. Laudise, R. A., and Nielsen, J. W., Hydrothermal Crystal Growth, in Solid State Physics, Vol. 12, Academic Press, New York-London, 1961.
10. These two experiments were carried out in the laboratories of Dr. Archie Deutschman, 4040 N. Campbell Ave., Tucson, with his generous cooperation.
11. Shafer, M. W., and Roy, Rustrum, J. Am. Cer. Soc., 12, No. 11, 563 (1959).
12. Prandtl et. al., Z. Anorg. Chem., 14, 235 (1925) and 238, 225 (1938).
13. Penneman and Asprey, private communication.
14. Makarov, S. Z., and Soboleva, L. V., (Chem. Abstr. 61:3889) Redkozem. Elementy, Akad. Nauk, SSSR, Just. Geokhemic. Analit. Khim. 1963, 61-66.
15. Bisi, C. A., and Clerici, A., Gazz. Chim. Ital., 93 (11) 1438 (1963).